Article

Cell

DNA Methylation on N^6-Adenine in *C. elegans*

Graphical Abstract

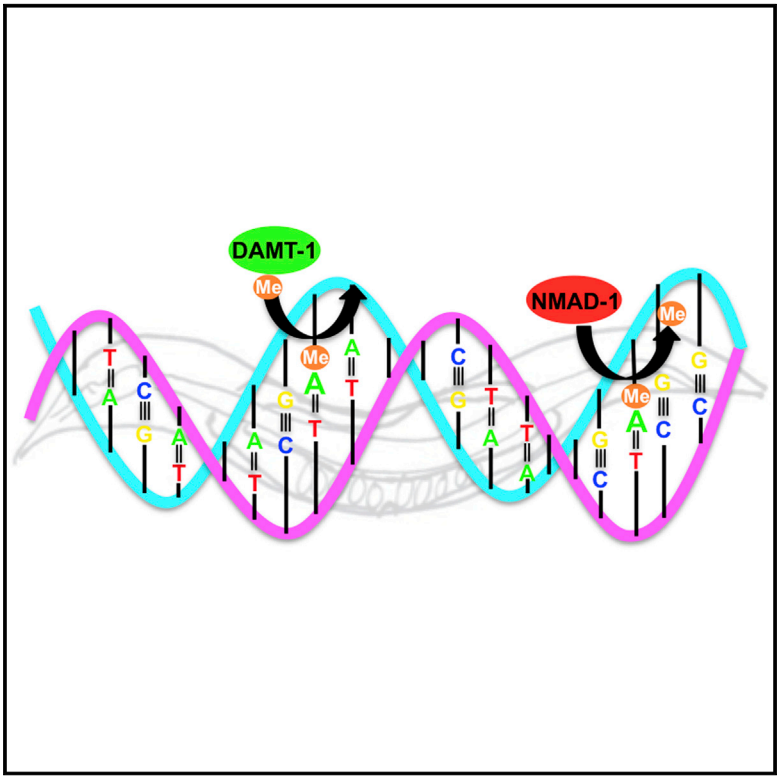

Authors

Eric Lieberman Greer,
Mario Andres Blanco, ..., Chuan He,
Yang Shi

Correspondence

eric.greer@childrens.harvard.edu
(E.L.G.),
yshi@hms.harvard.edu (Y.S.)

In Brief

Methylation is discovered to exist in *C. elegans* DNA on N^6-adenines, along with a demethylase and putative methyltransferase. These enzymes are involved in trans-generational epigenetic signaling, raising the exciting possibility that this methyl mark may have an epigenetic role.

Highlights

- Identification of adenine N6 methylation (6mA) on DNA in *C. elegans*
- Examination of 6mA distribution
- Identification of a 6mA DNA demethylase and its role in epigenetic inheritance
- Identification of a potential 6mA DNA methylase and its role in epigenetic inheritance

Greer et al., 2015, Cell *161*, 1–11
May 7, 2015
http://dx.doi.org/10.1016/j.cell.2015.04.005

CellPress

Please cite this article in press as: Greer et al., DNA Methylation on N^6-Adenine in *C. elegans*, Cell (2015), http://dx.doi.org/10.1016/j.cell.2015.04.005

Cell

DNA Methylation on N^6-Adenine in *C. elegans*

Eric Lieberman Greer,[1,2,5,*] Mario Andres Blanco,[1,2,5] Lei Gu,[1,2] Erdem Sendinc,[1,2] Jianzhao Liu,[3] David Aristizábal-Corrales,[1,2] Chih-Hung Hsu,[1,2] L. Aravind,[4] Chuan He,[3] and Yang Shi[1,2,*]

[1]Division of Newborn Medicine, Children's Hospital Boston, 300 Longwood Avenue, Boston, MA 02115, USA

[2]Department of Cell Biology, Harvard Medical School, Boston, MA 02115, USA

[3]Department of Chemistry and Institute for Biophysical Dynamics, Howard Hughes Medical Institute, The University of Chicago, Chicago, IL 60637, USA

[4]National Center for Biotechnology Information, National Library of Medicine, National Institutes of Health, Bethesda, MD 208943, USA

[5]Co-first author

*Correspondence: eric.greer@childrens.harvard.edu (E.L.G.), yshi@hms.harvard.edu (Y.S.)

http://dx.doi.org/10.1016/j.cell.2015.04.005

SUMMARY

In mammalian cells, DNA methylation on the fifth position of cytosine (5mC) plays an important role as an epigenetic mark. However, DNA methylation was considered to be absent in *C. elegans* because of the lack of detectable 5mC, as well as homologs of the cytosine DNA methyltransferases. Here, using multiple approaches, we demonstrate the presence of adenine N^6-methylation (6mA) in *C. elegans* DNA. We further demonstrate that this modification increases trans-generationally in a paradigm of epigenetic inheritance. Importantly, we identify a DNA demethylase, NMAD-1, and a potential DNA methyltransferase, DAMT-1, which regulate 6mA levels and crosstalk between methylations of histone H3K4 and adenines and control the epigenetic inheritance of phenotypes associated with the loss of the H3K4me2 demethylase *spr-5*. Together, these data identify a DNA modification in *C. elegans* and raise the exciting possibility that 6mA may be a carrier of heritable epigenetic information in eukaryotes.

INTRODUCTION

An increasing number of complex phenotypes, including physical appearance (Cavalli and Paro, 1998; Morgan et al., 1999), energy metabolism (Benyshek et al., 2006), behavioral state (Dias and Ressler, 2014), and longevity (Greer et al., 2011; Rechavi et al., 2014), have been shown to be regulated in part by non-genetic information. The molecular nature of the epigenetic information that is transmitted from generation to generation is still incompletely understood. It has been postulated that anything in the zygote that is not the DNA sequence itself could carry this non-genetic information. This includes proteins, non-coding RNA, and modifications to both proteins and DNA in chromatin (Greer and Shi, 2012; Martin and Zhang, 2007; Moazed, 2011). Arguments have been made for each of these modes of epigenetic inheritance, and it is possible that a given mode of inheritance may play a larger role than others, depending on the paradigm of inheritance. One paradigm of epigenetic inheritance in *C. elegans* involves mutation of the histone H3 lysine 4 dimethyl (H3K4me2) demethylase *spr*-5 (Katz et al., 2009), which is an ortholog of the mammalian LSD1/KDM1A (Shi et al., 2004). The *spr-5* mutant worms initially do not exhibit phenotypes; however, after successive generations lacking this demethylase, they display a progressively increased infertility. This fertility decline is concomitant with a global increase in the activating histone mark H3K4me2 and decline in the repressive histone mark H3K9me3 (Greer et al., 2014; Katz et al., 2009; Kerr et al., 2014; Nottke et al., 2011). Despite the fact that early- and late-generation *spr-5* mutant worms should be genetically identical, late-generation *spr-5* mutant worms display altered phenotypes, most likely because of the inheritance of non-genetic information.

Previous studies searched for DNA modifications that carry epigenetic information in *C. elegans.* An early report performed high-performance liquid chromatography (HPLC) on *C. elegans* as they age and suggested that *C. elegans* have 5-methylcytosine (5mC) and that it accumulates with age (Klass et al., 1983). Other nematode species have also been reported to have 5mC (Gao et al., 2012); however, subsequent studies in *C. elegans* were unable to replicate this finding (Simpson et al., 1986). This lack of reproducibility, coupled with the fact that *C. elegans* do not contain homologs of the enzymes that add methyl moieties to cytosine—DNA (cytosine-5-)-methyltransferase 1 (DNMT1) or DNMT3—has led to the prevailing view that *C. elegans* do not possess DNA methylation (Wenzel et al., 2011). However, DNA is not only methylated at the fifth position of the pyrimidine ring of cytosines. Other DNA methylation events have been reported, including methylation of the exocyclic NH_2 groups at the sixth position of the purine ring in adenines (6mA) and at the fourth position of the pyrimidine ring in cytosines (4mC) (Iyer et al., 2011). In prokaryotes, 4mC and 6mA are primarily used for distinguishing self from foreign DNA (Iyer et al., 2011). These modifications are considered to be signaling or epigenetic modifications because they are predicted not to disrupt DNA base pairing (Iyer et al., 2011). Conversely, methylations of the first position of the purine ring in adenines (1mA) and the third position of the pyrimidine ring in cytosines (3mC) are considered DNA damage methylation events because they disrupt the hydrogen bonding with their base pairs. Additional DNA modifications have also been discovered or predicted in bacteria and eukaryotes (Iyer et al., 2011, 2013), but it remains

to be seen whether they are conserved across all species. Studies in eukaryotic organisms typically focus on 5mC and its role as an epigenetic modification (Koh and Rao, 2013; Martin and Zhang, 2007). However, it remains unknown whether DNA modifications such as 6mA and 4mC can also be used as epigenetic marks in eukaryotes and potentially even perpetuated through cell divisions and generations via the semi-conservative nature of DNA replication.

Here, we demonstrate that 6mA occurs in *C. elegans* DNA, is broadly distributed across the genome, and increases trans-generationally in *spr-5* mutant worms. We identify a 6mA DNA demethylase, NMAD-1, and show that deletion of *nmad-1* accelerates the progressive fertility defect phenotype of *spr-5* mutant worms. Conversely, deletion of *damt-1*, a potential 6mA DNA methyltransferase, reduces 6mA levels in worms and suppresses the progressive fertility defect of *spr-5* mutant worms. Additionally, we also identify reciprocal regulation between DNA 6mA and histone methylation. Our study identifies a new DNA modification in *C. elegans*, as well as regulators that control the dynamics of this modification, and advances 6mA as a potential carrier of non-genetic information across generations.

RESULTS

6mA Occurs in *C. elegans* and Increases Trans-generationally in *spr-5* Mutant Worms

To investigate whether any forms of DNA methylation are present in *C. elegans* and could be potential carriers of epigenetic memory in worms lacking *spr-5*, we extracted genomic DNA (gDNA) from whole worms and performed dot blot analysis on wild-type (WT) and late-generation *spr-5*(*by101*) mutant worms using a number of DNA modification-specific antibodies. Excitingly, we found that (1) 6mA, but not 5mC or 5hmC, was detectable in gDNA from WT worms and (2) the level of 6mA appears to be elevated in *spr-5* mutant worms (Figure S1A). To exclude the possibility that the detected 6mA is due to contamination from bacterial DNA, which contains 6mA, we used a bacterial food source that was deficient in the DNA adenine methyltransferase (Dam) and DNA cytosine methyltransferase (Dcm) enzymes, which are responsible for 6mA and 5mC modifications in bacteria, respectively (we confirmed that this mutant bacterial strain does not contain 6mA [Figure S1B]). To exclude the possibility that the detected 6mA was due to contaminating methylated RNA, we treated purified gDNA with enzymes targeting all major forms of RNA, including RNase A, RNase T1, and RNase H. We found that gDNA extracted from WT and late-generation *spr-5* mutant worms fed with *dam*$^-$*dcm*$^-$ bacteria and treated with several RNases still exhibited detectable 6mA (Figure S1B). Furthermore, 6mA antibodies only detected very low signals from worm RNA dot blots, confirming that the observed 6mA DNA dot blot signals were not derived from potentially contaminating RNA in our genomic DNA preparations (Figures 1A and S1C). Lastly, we detected 6mA in worm gDNA samples using 6mA antibodies from two independent sources (Figures S1A and S1B).

We confirmed the specificity of the antibodies used in our dot blot analysis using a panel of unmethylated and premethylated DNA oligos (Figure S1D). Two 6mA antibodies (Synaptic Systems and Megabase) recognized either single- or double-stranded 6mA- but not 3mC-containing oligos. The 6mA antibodies also recognized the non-denatured (double-stranded, ds), but not denatured (single-stranded, ss), 1mA (Figure S1D). Because the worm gDNA was denatured before being loaded onto blots, the 6mA antibody-detected signal was likely N^6 adenine methylated DNA.

The elevation of 6mA in late generation *spr-5* mutant worms raises the possibility that 6mA might potentially play a role in transmitting heritable epigenetic information. Therefore, we next investigated whether the 6mA level changes in a trans-generational manner, as *spr-5* mutant worms have been shown to display a trans-generational increase in H3K4me2 level concomitant with trans-generational fertility defects (Greer et al., 2014; Katz et al., 2009). We found that 6mA increased in a trans-generational manner in *spr-5* mutant worms, regardless of worm culturing temperatures (Figure 1A). The magnitude of the increase in 6mA was variable across biological replicates, but the trend toward more 6mA in *spr-5* mutant worms was consistent.

To confirm that we were detecting 6mA, we turned to an antibody-independent approach, i.e., ultra-high-performance liquid chromatography coupled with a triple-quadrupole tandem mass spectrometry (UHPLC-MS/MS) analysis. We found that 6mA levels were variable from experiment to experiment in WT worms (occurring on between 0.01%–0.4% of adenines). However, 6mA levels were invariably elevated in the *spr-5*(*by101*) mutant worms, though the degree of upregulation differs from experiment to experiment (between 1.5- and 17-fold) and depends on the generation of worms assayed (Figure 1B and data not shown).

We initially noted that 1mA appeared to also increase in *spr-5* mutant worms as detected by the 1mA antibody (Figure S1C). However, the 1mA antibody recognizes both 1mA and 6mA oligos and therefore cannot distinguish the two modifications (Figure S1D), whereas UHPLC-MS/MS readily separates 1mA and 6mA (Figure S2). UHPLC-MS/MS analysis of WT and *spr-5* mutant worms gDNA typically failed to detect any 1mA in either strain (Figure S2B), indicating that the changes observed with our 1mA antibody likely reflected recognition of the elevated 6mA levels. On one occasion (out of more than ten trials) in which 1mA was detected by UHPLC-MS/MS, it was observed to be at similarly low levels in WT and *spr-5* mutant worms (Figure S1E).

We next investigated tissue distributions of 6mA by performing immunofluorescence (IF) on extracted germlines, embryos, and whole worms (Figures 1C, 1D, and S3A), which had been treated with RNases to remove potential RNA 6mA signal. We found 6mA present ubiquitously throughout the worm except for sperm nuclei (Figures 1C and S3A) and in every other cell in the worms' germline (Figure 1D). The absence of 6mA in sperm (Figure 1C) could reflect the high compaction of sperm chromatin (which might hamper the antibody accessibility) or could be indicative of a paternal erasure of 6mA. The IF signal likely represents 6mA, as pre-incubation of the antibodies with 6mA oligos, but not unmethylated oligos, abrogated the nuclear signal and resulted in a diffused, non-specific staining (Figure 1D). We also detected 6mA signal ubiquitously throughout the embryo (Figure 1C). Whereas 6mA was elevated in *spr-5* mutant worms

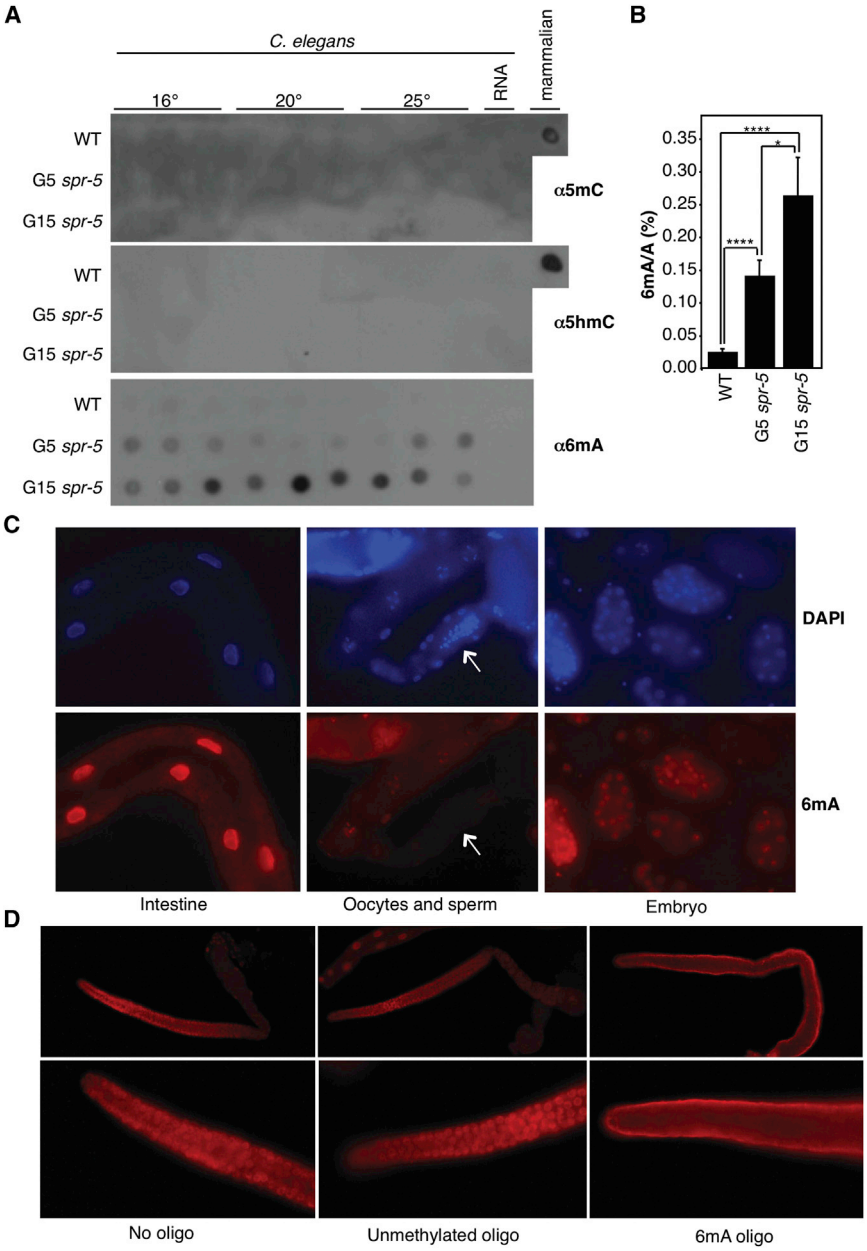

Figure 1. 6mA Occurs in *C. elegans* DNA and Increases across *spr-5* Generations

(A) Dot blots of three biological replicates of WT, generation 5, and generation 15 *spr-5*(*by101*) mutant worms grown at 16°, 20°, or 25° all show progressively elevated 6mA and lack detectable 5mC and 5hmC. 250 ng of gDNA are loaded per dot. Mammalian gDNA is used as a control for 5mC and 5hmC antibody strength.

(B) 6mA levels increase across generations of *spr-5*(*by101*) mutant worms as assessed by UHPLC-MS/MS. Each column represents the mean and SD of three to five biological replicates per group. *$p < 0.05$ and ****$p < 0.0001$.

(C) Immunofluorescence displays 6mA staining in the intestine, oocytes, and every cell of the embryo. Arrow indicates sperm.

(D) Immunofluorescence of wild-type extracted germlines shows 6mA in every nuclei. This staining was competed by a 6mA premethylated oligo but not by unmethylated oligos.

See also Figures S1, S2, and S3.

(Figure S3A), 3mC and 1mA signals were essentially undetectable in germlines extracted from generation 20 (G20) *spr-5*(*by101*) mutant and WT worms (Figure S3B).

To determine whether 6mA might be associated with DNA damage, we performed dot blot analysis and stained gonads extracted from WT and DNA damage-deficient mutant strains. We found that deletion of the DNA damage genes, *xpa-1* (UV damage), *ercc-1* (nucleotide excision repair), and *sod-2* and *sod-3* (oxidative stress) did not lead to appreciably altered levels of 6mA (Figures S4A and S4B), nor did treatment with lethal doses of the DNA damaging agent methyl methanesulfonate (MMS) (Figure S4C). Together, these results suggest that 6mA is not a DNA damage-induced modification.

6mA Genomic Locations

For an initial investigation of 6mA genomic localization, we performed 6mA methylated DNA immunoprecipitation (Figure S5A), followed by sequencing (MeDIP-seq) on mixed-stage WT worms. MeDIP-seq identified 766 6mA peaks broadly distributed throughout the genome and evenly represented across major genomic features, except for a modest depletion in introns (Figure S5B). The most prevalent motif, AGAAGAAG AAGA, was present in 314 of the peaks identified ($p = 1e{-}42$, Figure S5C).

To more directly interrogate 6mA localization using an antibody-independent, base pair resolution approach, we carried out single-molecule real-time sequencing (SMRT sequencing), which not only identifies individual bases but also their modifications (Flusberg et al., 2010). We generated a SMRT sequencing dataset, using gDNA from mixed-stage, WT worms. To increase our read density, we merged our dataset with the publicly available *C. elegans* SMRT sequencing data generated by Pacific Biosciences (http://datasets.pacb.com.s3.amazonaws.com/2014/c_elegans/list.html). In this analysis, SMRT sequencing detected 6mA on 225,586 adenines—~0.7% of the total adenines in the worm genome—which is equivalent to 0.3% bulk adenine methylation, as some adenines were methylated 10% of the time, whereas others were methylated 90% of the time. This value (0.3%) is comparable to some of the UHPLC-MS/MS results (Figure 5E). SMRT sequencing does not distinguish 6mA versus 1mA, but 1mA is rarely above the level of detectability by UHPLC-MS/MS in worm gDNA. This suggests that the signals detected through SMRT sequencing

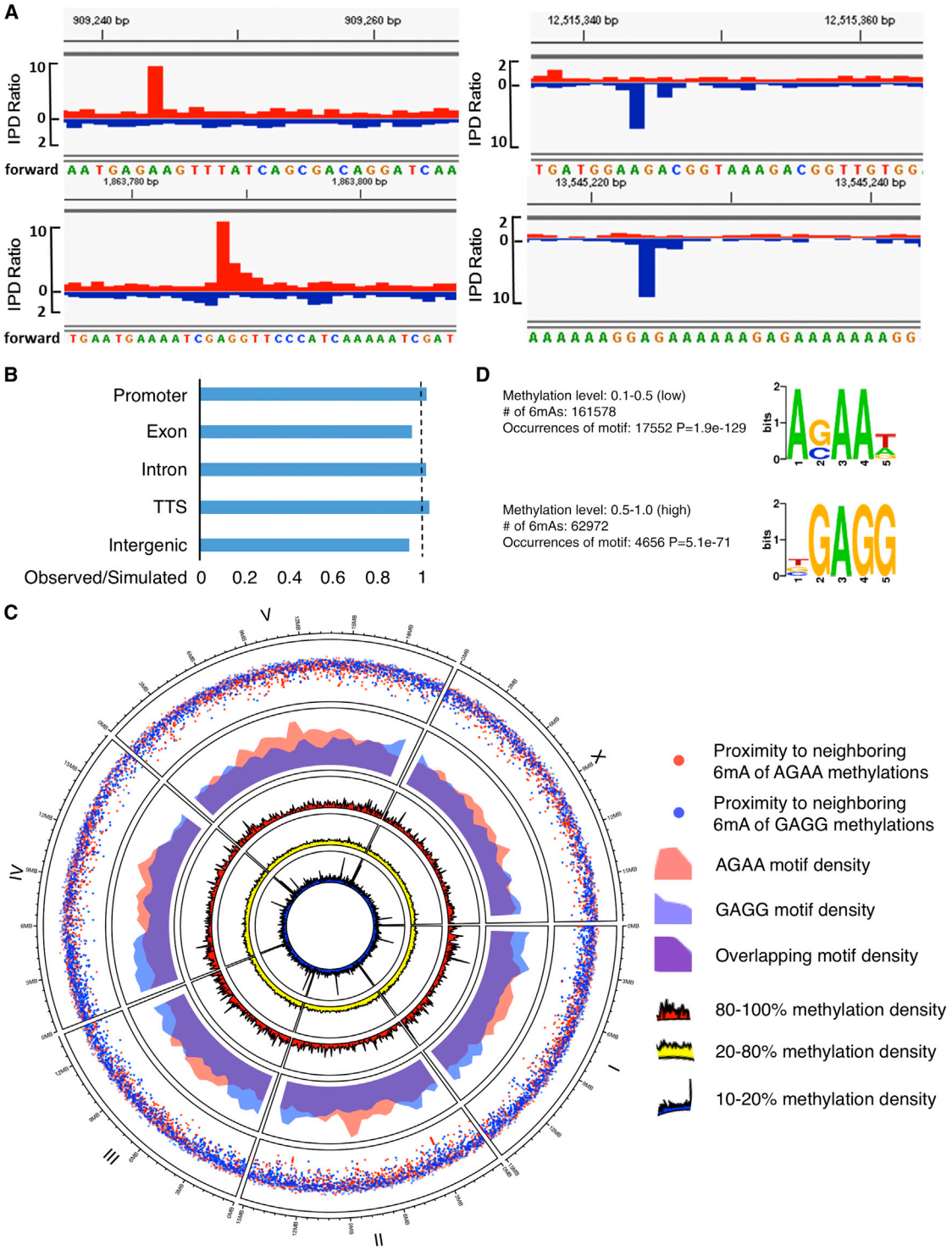

Figure 2. 6mA Genomic Location

(A) Representative interpulse duration (IPD) ratios of SMRT sequencing data of mixed-stage WT worms. IPD ratio is defined as the change in IPD distribution in the sample compared to unmodified bases. Red, positive strand; blue, negative strand.

(B) Comparison of observed versus simulated distributions of 6mA across the *C. elegans* genome indicates that 6mA is not enriched or depleted in any major genomic feature. A permutation was used to calculate the average of 10,000 simulations for comparison to the observed data.

(C) Circos plots of 6mA and motif distributions; three inner rings: 6mA density normalized to adenines in each bin of 6mAs within different methylation fractions. Red, yellow, and blue represent highly methylated (80%–100%), intermediate (20%–80%), and lowly methylated (10%–20%) 6mA, respectively. The middle ring

(legend continued on next page)

were 6mA (Figure 2A), although we cannot completely exclude the possibility that rare occurrences of 1mA could have been detected as 6mA in our SMRT sequencing analysis. Similar to the MeDIP-seq results, the SMRT sequencing analysis identified a broad distribution of 6mA across all chromosomes of the worm genome, with no one genomic feature being significantly enriched or depleted for 6mA (Figures 2B and 2C). Because lowly methylated regions usually include functional elements in mammalian cells (Stadler et al., 2011), we examined 6mA distribution (Figure 2C) by separating it into low (10%–20%, dark blue circle), middle (20%–80%, yellow circle), and high (80%–100%, red circle) categories and presenting the data in circos plot format in which concentric rings represent the density distributions of 6mA across the six worm chromosomes in the given category. We found that some lowly methylated regions appeared in dense clusters similar to lowly methylated 5mC (Figure 2C, innermost concentric circle). Notably, two sequence motifs were significantly associated with the presence of 6mA (Figure 2D): AGAA ($p = 1.9e{-}129$) and GAGG ($p = 5.1e{-}71$). Importantly, the AGAA motif identified by SMRT sequencing was also identified by MeDIP-seq (Figure S5C). Interestingly, the GAGG motif was most prevalent in sites that were frequently 6mA methylated (50%–100% methylation level), whereas the AGAA motif was most prevalent in infrequently 6mA methylated sites (10%–50% methylation level). The two 6mA motifs did not significantly differ in chromosomal distribution (Figure 2C, fourth concentric circle), though there were some regions that showed increased clustering density for each of the 6mA motifs (Figure 2C, outer rainfall plot). Notably, both motifs indicate that methylation at these sites occurs only on one of the strands, unlike the strong propensity for 5mC to occur in the context of CG doublets in various eukaryotes. Both SMRT sequencing and MeDIP-seq—which have been performed on mixed tissues and mixed-stage worms—confirmed the presence of 6mA in worm DNA across the genome and at similar sequence motifs.

Deletion of Potential Dealkylating Enzyme, *nmad-1*, Accelerates the Progressive Fertility Defect of *spr-5* Mutant Worms

To identify the enzymes responsible for the addition and removal of 6mA in *C. elegans*, we first examined the ALKB family of dealkylating enzymes, which have been shown in other species to remove methyl groups from DNA and RNA oxidatively, utilizing 2-oxoglutarate as a cofactor (Yi and He, 2013). Because 6mA levels increased across generations of *spr-5* mutant worms, we hypothesized that deletion of a 6mA demethylase would accelerate the trans-generational fertility defect of *spr-5* mutant worms. To determine whether any of the five *C. elegans* ALKB family members (Figure 3A) regulates 6mA, we first investigated whether knockdown or deletion of the family members had any effect on the progressive fertility defect of *spr-5* mutant worms. We found that knockdown of *Y51H7C.1*, *B0564.2*, *Y46G5A.35*, and *C14B1.10* had no effect on the fertility of WT or *spr-5* mutant worms (Figures 3B and S6A). Although we were unable to efficiently knock down the fifth ALKB family member, *F09F7.7* (Figure S6A), we obtained a worm strain carrying a deletion of *F09F7.7*(*ok3133*) and found that loss of *F09F7.7* accelerated the progressive fertility defect of *spr-5* mutant worms such that the *spr-5;F09F7.7* double-mutant worms became completely sterile by generation 4 (Figure 3C). As a control, we found that, at a similar generation, the *spr-5* mutant worms did not display a significant fertility defect (Figure 3A; Greer et al., 2014; Katz et al., 2009). As a further control, we examined and found that *F09F7.7* mutants laid fewer eggs than WT worms (Figure 3C), but, importantly, this phenotype was not progressive (Figure 3D), suggesting that the acceleration of the progressive fertility defect of *spr-5* mutant worms is a result of a specific genetic interaction between *F09F7.7* and *spr-5*. These findings suggested that F09F7.7 may act as a 6mA demethylase in vivo, which is further supported by the biochemical experiments discussed below. We thus renamed F09F7.7 N6-methyl adenine demethylase 1 (*nmad*-1) to reflect this newly identified function.

NMAD-1 Demethylates 6mA In Vitro and In Vivo

To biochemically determine whether NMAD-1 was a 6mA demethylase, we glutathione S-transferase (GST) tagged and purified the protein and tested its demethylating activity in vitro. We found that two different isoforms of NMAD-1 were able to demethylate 6mA and 3mC oligos but not 1mA oligos in vitro (Figure 4A). To determine whether this demethylating activity was intrinsic to NMAD-1, we mutated the iron-chelating aspartic acid 186 in the catalytic domain of NMAD-1 to an alanine (D186A) and found that this mutation abrogated the ability of NMAD-1 to demethylate 6mA oligos (Figure 4B), suggesting that NMAD-1 possesses 6mA demethylase activity in vitro. We next investigated whether *nmad-1* mediates demethylation of both 6mA and 3mC in vivo. As shown in Figure 4C, *nmad-1* mutant worms showed elevated levels of 6mA, but not 3mC. This elevated 6mA was further confirmed by UHPLC-MS/MS (Figure 4D). Together, these results suggest that NMAD-1 is primarily a 6mA demethylase in vivo, although recombinant NMAD-1 protein can demethylate both 6mA and 3mC in vitro.

Deletion and Overexpression of the Potential Methyltransferase *damt-1* Decreases and Increases 6mA Levels In Vivo and in Tissue Culture, Respectively

We next sought to identify enzymes that mediate adenine N^6-methylation in *C. elegans*. Although candidate 6mA DNA methyltransferases have been identified in chlorophyte algae, ciliates, some fungi, and certain other eukaryotic lineages (Iyer et al., 2011, 2014), none have been identified in Metazoa thus far. Although the eukaryotic candidate 6mA methyltransferases

shows AGAA (red) and GAGG (blue) motif densities, with purple indicating the overlap. The outer ring (rainfall plot) shows the distribution of inter-distance between each two adjacent 6mAs in the same motif. Red dots represent 6mAs in AGAA motif, and blue dots represent 6mAs in GAGG motif; increasing vertical distance toward the center of the circle indicates increasing local density of 6mA occurrences.

(D) SMRT sequencing identified two motifs associated with 6mA. AGAA and GAGG are associated with low- and high-percentage 6mA, respectively. Methylation level refers to the percentage of times (1.0 = 100%) a given A in the sample population was read as methylated by SMRT sequencing.

See also Figure S5 for 6mA MeDIPseq.

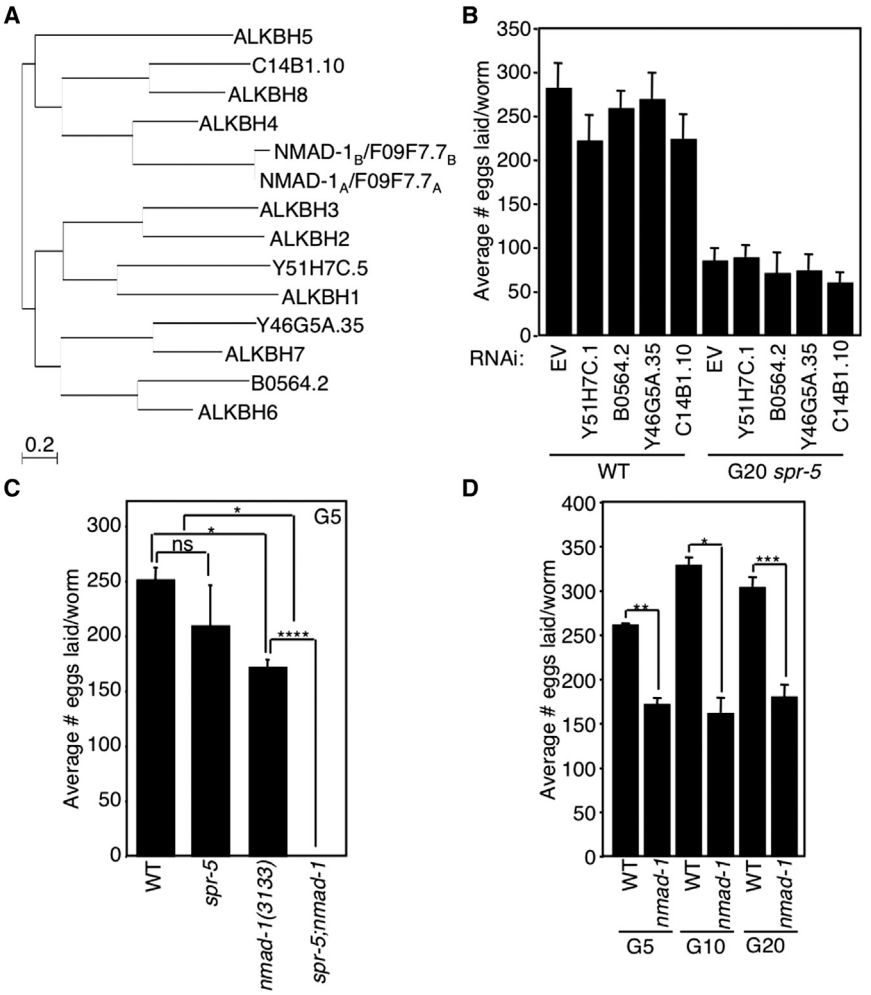

Figure 3. Deletion of *nmad-1* Accelerates the Progressive Fertility Defect of *spr-5* Mutant Worms

(A) Phylogeny tree of human and *C. elegans* ALKBH family members.

(B) Knockdown of 4 of the ALKBH family members has no effect on egg laying of WT and *spr-5* mutant worms treated for 20 generations with bacteria expressing the specific dsRNAs. Knockdown efficiency was tested by real-time RT-PCR (Figure S6A).

(C) Early-generation (G5) *spr-5* mutant worms do not display significant fertility defects, but when combined with *nmad-1* deletion, these worms become sterile by generation 4. Each bar represents the mean ± SEM of three independent experiments.

(D) *nmad-1* mutants lay fewer eggs than WT worms but do not display a progressive fertility decline. Each bar represents the mean ± SEM of two to six independent experiments. *p < 0.05, **p < 0.01, ***p < 0.001, and ****p < 0.0001; ns, not significant.

belong to multiple distinct methylase lineages (Iyer et al., 2011), the most widespread versions belong to the MTA-70 family exemplified by the yeast mRNA adenine methylase complex Ime4/Kar4 (Anantharaman et al., 2002; Clancy et al., 2002). These enzymes have evolved from m.MunI-like 6mA DNA methyltransferases of bacterial restriction-modification systems (Iyer et al., 2011) and are typified by a C-terminal circularly permuted methyltransferase domain fused to a distinctive N-terminal, predicted α-helical domain with a strongly positively charged segment. *C. elegans* has one representative of this family—the gene *C18A3.1*, which is conserved across eukaryotes, including humans, plants, basal fungi, certain amoebozoans, and stamenopiles and can be distinguished by phylogenetic analysis from Ime4 and Kar4 that are absent in *C. elegans* (Figures 5A and S6B). The orthologs of C18A3.1 form a distinct clade, separated from the mRNA methylase complex clade, within the primary eukaryotic radiation of the MTA-70 family. *C. elegans* also lack the transposon-encoded 6mA DNA methylase domains, which are found in related nematodes like *C. remanei.* These observations suggest that C18A3.1 is the primary 6mA DNA methylase candidate in *C. elegans.*

We investigated whether C18A3.1 could methylate the sixth position of adenines, but due to its high hydrophobicity, we were unable to purify this protein from bacterial or insect cells in sufficient quantities to study its activity in vitro. However, when we analyzed the gDNA isolated from SF9 cells expressing full-length C18A3.1 or the catalytic domain of C18A3.1 alone, we found that 6mA levels were elevated compared to DNA from insect cells that do not express C18A3.1 (Figure 5B). To determine whether this potential methylating activity was intrinsic to C18A3.1, we mutated amino acids in the N6A methyltransferase signature (DPPW) important for substrate recognition and catalytic activity (Iyer et al., 2011) and found that mutation of DPPW to APPA in the catalytic domain ablated the 6mA induction in SF9 gDNA (Figures 5C and S6C). This result suggests that C18A3.1 (renamed *damt-1* for DNA N6 adenine methyltransferase 1) is itself a 6mA methyltransferase, although we cannot rule out the less likely possibility that C18A3.1 expression in insect cells coincidentally activated an endogenous insect cell enzyme that is responsible for the observed 6mA. To determine whether DAMT-1 was a 6mA methyltransferase in vivo, we knocked down *damt-1* in WT worms and found decreased 6mA but not 3mC levels in the extracted gDNA (Figures 5D and 5E). *damt-1* knockdown also decreased 6mA levels in *spr-5*(*by101*) mutant worms to similar levels as in WT worms (Figure 5F). Taken together, these data suggest that DAMT-1 is a 6mA methyltransferase in *C. elegans*.

Deletion of *damt-1* Suppresses the Trans-generational Phenotypes of *spr-5* Mutant Worms

If DAMT-1 is a 6mA methyltransferase, then we would expect that its knockdown or deletion would suppress the trans-generational phenotypes of *spr-5* mutant worms. Indeed, knockdown of *damt-1* for 20 generations partially suppressed the progressive fertility

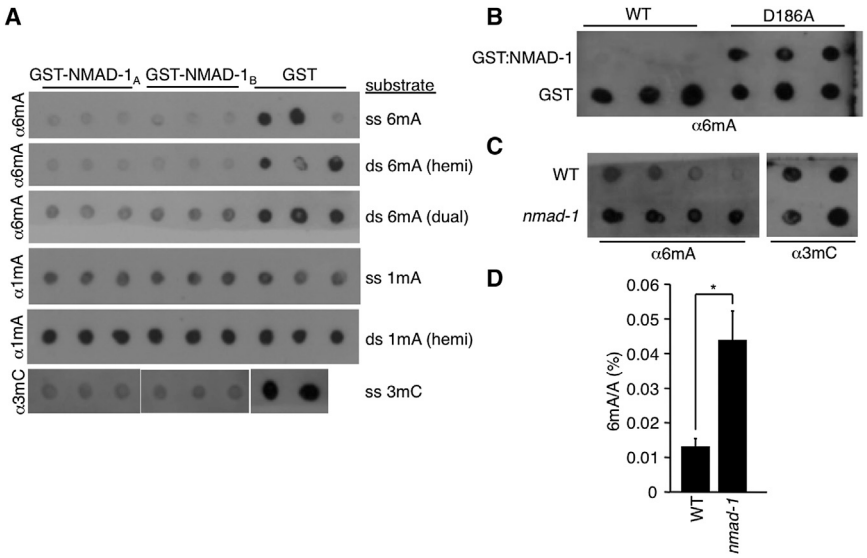

Figure 4. NMAD-1 Demethylates 6mA In Vitro and In Vivo

(A) Two different isoforms of NMAD-1 demethylate ss-denatured and ds-non-denatured (hemi or dual methylated) oligos premethylated at 6mA and 3mC but not 1mA.

(B) Mutation of the catalytic domain of NMAD-1 abrogates the ability of NMAD-1 to demethylate 6mA premethylated oligos.

(C) *nmad-1* mutants have elevated levels of 6mA without detectable changes in 3mC levels. Each dot represents 250 ng of DNA of independent biological replicates.

(D) *nmad-1* mutants have elevated levels of 6mA as assessed by UHPLC-MS/MS. Each bar represents the mean and SE of the mean of two independent biological replicates measured in duplicate. *$p < 0.05$.

defect of *spr-5*(*by101*) mutant worms without affecting the fertility of WT worms (Figure 6A). Specifically, late-generation *spr-5* mutant worms on *damt-1* RNAi laid two to three times more eggs than late-generation *spr-5* mutant worms on bacteria containing an empty RNAi vector (Figure 6A). Similarly, a genetic deletion (gk961032) that removes the entirety of *damt-1* and a portion of the nearby Ras GTPase superfamily gene *rab-3* had no effect on egg laying by itself but suppressed the progressive fertility defect of *spr-5*(*by134*) mutant worms at generations 10, 17, 20, and 26 (Figure 6B and data not shown). *damt-1* knockdown also eliminated the fertility defect of the *nmad-1* mutant worms, suggesting that DAMT-1 functions to counteract the activity of the 6mA demethylase, NMAD-1, in vivo (Figure 6C). Collectively, these data suggest that DAMT-1 is a 6mA methyltransferase that suppresses the trans-generational phenotypes of *spr-5* mutant worms.

Crosstalk between H3K4me2 and 6mA

As discussed earlier, we initially observed an increase in 6mA levels in the histone H3K4me1/me2 demethylase mutant *spr-5*. Conversely, we found that deletion of the potential 6mA methyltransferase, *damt-1*, reduced the elevated H3K4me2 levels of *spr-5* mutant worms (Figures 7A, S7A, and S7B). Furthermore, we found that knockdown of the H3K9me binding protein *eap-1*, which reduces H3K4me2 levels in *spr-5* mutant worms (Greer et al., 2014), also reduced the levels of 6mA in *spr-5* mutant worms (Figures 7B and S7C). Collectively, these findings suggest reciprocal regulation of H3K4 and adenine N^6 methylation and crosstalk between regulators that control adenine and histone methylation.

DISCUSSION

To date, 6mA has primarily been studied in prokaryotes, where it has been shown as a mark to discriminate invasive DNA (Arber and Dussoix, 1962; Meselson and Yuan, 1968). However, prokaryotic 6mA also functions as a binding platform and influences gene expression (Braun and Wright, 1986; Han et al., 2004). 6mA has also been reported in more ancient eukaryotes such as ciliates, in which it is observed in the macro (somatic) and not in the micro (germline) nucleus, highlighting its potential function in a broad range of biological contexts (Gutiérrez et al., 2000). Both fungi and animals are known to undergo methylation of adenosine in mRNA, with 6mA influencing mRNA stability (Fu et al., 2014) and RNA splicing (Dominissini et al., 2012; Liu et al., 2015). However, whether 6mA is present in DNA of Metazoa has been unclear, and it has been widely assumed that 5mC, rather than 6mA, plays a primary role as the key carrier of epigenetic information on DNA in these organisms (Wion and Casadesús, 2006). Importantly, this study not only identifies the presence of 6mA in *C. elegans* but also raises the exciting possibility that this modification may play a role in carrying and transmitting epigenetic information across generations, and that, in addition to 5mC, 6mA may also be used across eukaryotes as a potential epigenetic modification.

Our conclusion that 6mA is present in the *C. elegans* genome is supported by multiple lines of evidence. First, 6mA was detected by two independently developed 6mA-specific antibodies (Figures 1A and S1A). Second, 6mA was detected on the DNA of most cells throughout the worm by immunofluorescence (Figures 1C, 1D, S3, and S4A). Third, the presence of 6mA was also identified by an antibody-independent means, i.e., UHPLC-MS/MS, which showed that *C. elegans* genome possesses 6mA (Figure 1B). Fourth, two independent sequencing methods—direct, antibody-independent DNA sequencing using SMRT sequencing and the antibody-dependent MeDIPseq—both detected 6mA on *C. elegans* DNA (Figures 2 and S5). Although both sequencing methods have caveats about distinguishing between 1mA and 6mA, the DNA samples subjected to sequencing had undetectable 1mA (as determined by UHPLC-MS/MS), suggesting that the majority of the methylation events detected by SMRT sequencing likely represent 6mA. Finally, we also identified potential enzymatic machineries that mediate addition and removal of 6mA (Figures 4 and 5). Importantly, manipulation of these enzymes in vivo not only affects 6mA levels but also impacts trans-generational epigenetic inheritance

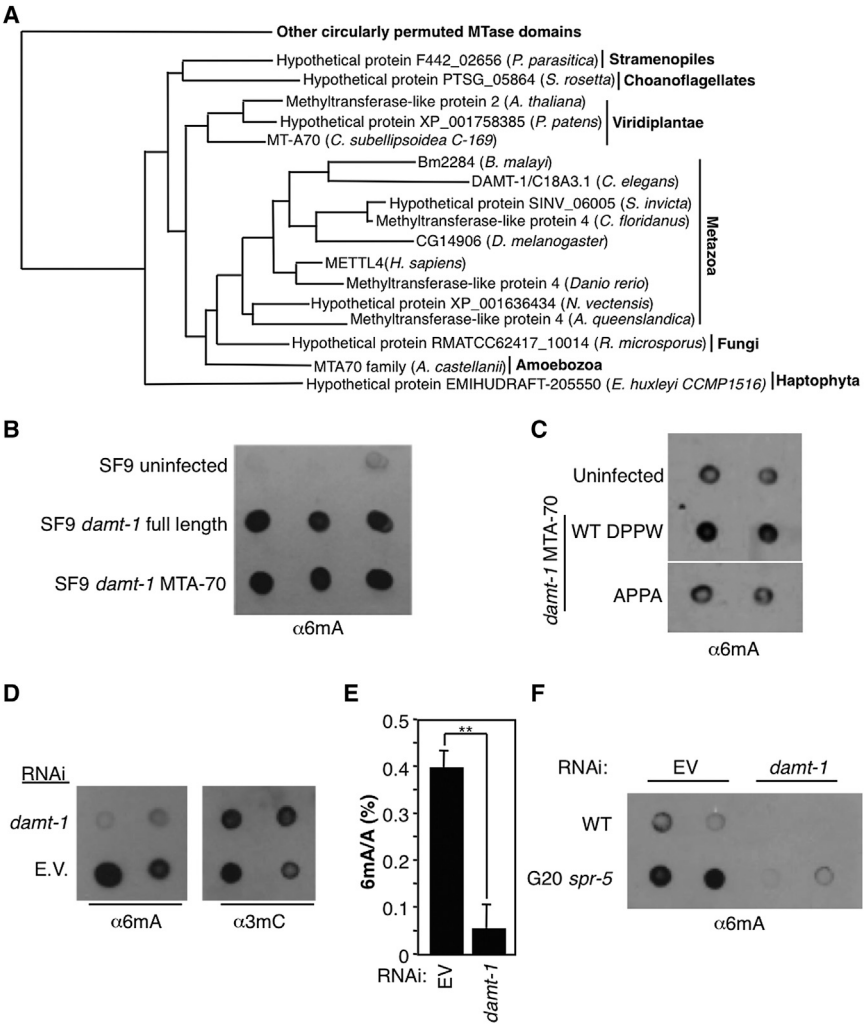

Figure 5. DAMT-1 Regulates 6mA Levels

(A) Phylogeny tree shows conservation of DAMT-1 in other eukaryotic species. Full tree and details of related clades are presented in Figure S6B.

(B) gDNA extracted from SF9 cells infected with full-length or the catalytic domain of *damt-1* show elevated levels of 6mA by dot blot.

(C) Mutation of the catalytic domain of DAMT-1 (DPPW to APPA) limits the increase in 6mA levels of infected SF9 cells. DAMT-1 expression is presented in Figure S6C.

(D) *damt-1* knockdown decreases 6mA without affecting detectable 3mC levels.

(E) *damt-1* mutants have decreased levels of 6mA as assessed by LC-MS/MS. Each bar represents the mean and SEM of three independent experiments of three biological replicates, each measured in duplicate. **$p < 0.01$.

(F) Generation 20 (G20) *spr-5* mutant worms show elevated 6mA levels compared with WT worms, and *damt-1* knockdown suppresses the elevated 6mA in *spr-5* mutant worms. Each dot represents 250 ng of gDNA of independent biological replicates.

in *C. elegans* (Figures 3 and 6), raising the exciting and attractive possibility that 6mA may indeed carry epigenetic information.

Both SMRT sequencing and MeDIP-seq identified a broad 6mA genomic distribution with a common sequence motif but without a clear enrichment pattern; in contrast, 5mC distributions in mammals are highly tissue specific (Smith and Meissner, 2013). Given that worms of mixed developmental stages were used for sequencing, the possibility that 6mA may be enriched in specific genomic locations in a tissue-, cell-type-, or developmental-stage-specific manner remains, and such enrichment patterns may only emerge when DNA samples from specific cell types or developmental stages are analyzed.

Although DNA methylation may be a more efficient carrier of epigenetic information, it remains to be seen whether 6mA, H3K4me2, or some as-of-yet-unidentified mark carry the epigenetic information on their own or collaborate to transmit epigenetic information across generations in *C. elegans*. A recent study provided evidence that both the histone modification mark (H3K27me3) and the PRC2 machinery are transmitted across generations epigenetically (Gaydos et al., 2014), implicating chromatin modifications as possible carriers of heritable non-genetic information. Interestingly, our study identified robust genetic interactions between the H3K4me1/2-specific demethylase SPR-5 and machineries that regulate 6mA—i.e., NMAD-1 and DAMT-1—in the regulation of trans-generational epigenetic inheritance. These results suggest crosstalk between 6mA and histone methylation and possible collaboration of these modifications in transmitting epigenetic information. Further evidence for this crosstalk was provided by the finding that knockdown of the H3K9me binding protein, *eap-1*, which reduces H3K4me2 levels in *spr-5* mutant worms (Greer et al., 2014), also decreases 6mA levels in *spr-5* mutant worms (Figure 7B). Conversely, deletion of the potential 6mA methyltransferase, *damt-1*, decreases H3K4me2 levels in *spr-5* mutant worms (Figure 7A). Consistent with the possibility of crosstalk between H3K4 and adenine N^6 methylation regulation, analysis of the domain architectures of DNA N6A methyltransferases in eukaryotes, such as chlorophytes and fungi, showed that the DNA-modifying catalytic domain is fused to histone-recognition domains (Iyer et al., 2011, 2014).

At the present time, the molecular function of 6mA is still unclear. DNA methylation systems such as 6mA and 5mC are proposed to serve various functions, including protection of host genomes (Arber and Dussoix, 1962; Meselson and Yuan, 1968), silencing of transposable elements (Kato et al., 2003; Zemach and Zilberman, 2010), transcriptional silencing (Csankovszki et al., 2001; Sado et al., 2000; Stein et al., 1982), prevention of cryptic transcription in intragenic regions (Zemach et al., 2010), and heterochromatin state transitions (Saksouk et al.,

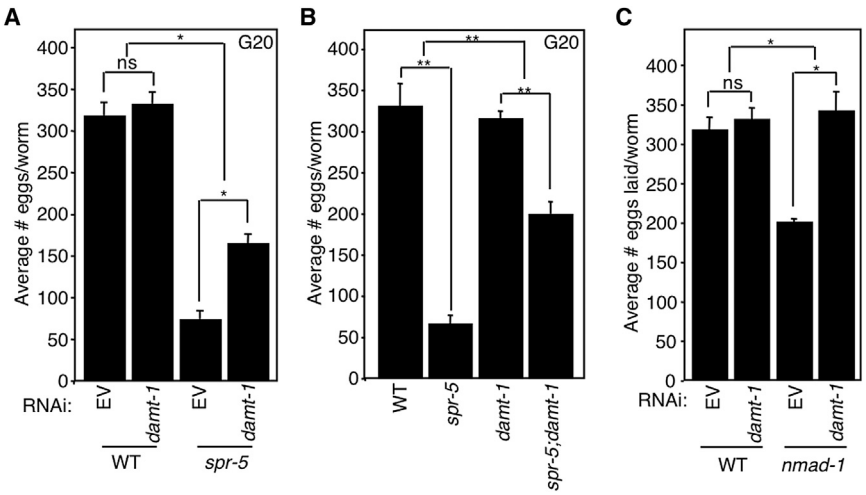

Figure 6. Deletion of *damt-1* Suppresses the Trans-generational Phenotypes of *spr-5* Mutant Worms

(A) *damt-1* knockdown has no effect on WT egg laying but partially suppresses the progressive fertility defect of *spr-5*(*by101*) mutant worms.

(B) *damt-1* deletion has no effect on WT egg laying but partially suppresses the progressive fertility defect of *spr-5*(*by134*) mutant worms.

(C) *damt-1* knockdown reverts the egg-laying defect of *nmad-1* mutant worms. All assays were performed at generation 20. Each bar represents the mean ± SEM of three independent experiments. *p < 0.05 and **p < 0.01; ns, not significant.

2014). A study conducted in *Chlamydomonas reinhardtii* (Fu et al., 2015 [this issue of *Cell*]) shows a correlation of 6mA modification with active gene transcription, suggesting a possible role in gene expression regulation. We observed that the absolute 6mA levels were variable from experiment to experiment and found that some environmental manipulations altered 6mA levels (data not shown). This raises the possibility that this modification could integrate environmental stimuli to regulate biological processes. Future studies will be required to fully explore the molecular function of 6mA in worms.

Finally, it will be informative to place 6mA regulation within a cellular pathway(s). In *Arabidopsis*, for example, the RNAi pathway feeds into 5mC regulation and heterochromatin formation and propagation (Law and Jacobsen, 2010; Teixeira et al., 2009; Wassenegger et al., 1994). Whether molecular pathways governing the trans-generational epigenetic inheritance of fertility and other phenotypes feed into 6mA regulation in *C. elegans* remains to be determined. It will be of significant interest to understand whether 6mA contributes to regulating the epigenome landscape that governs trans-generational epigenetic inheritance. Furthermore, given that orthologs of *damt-1* are widely conserved across eukaryotes, including mammals and other vertebrates, it will now be of great interest to investigate which other eukaryotic species might also have 6mA in their DNA and in which biological contexts this modification is regulated and plays a biological function. If other eukaryotes are found to have 6mA, it raises the exciting possibility that 6mA could carry epigenetic information in multiple paradigms of epigenetic inheritance.

EXPERIMENTAL PROCEDURES

Worm Strains

The N2 Bristol strain was used as the WT background. The following mutations were used in this study: LG1: *spr-5*(*by101*), *spr-5*(*by134*), *ercc-1*(*tm1981*), *xpa-1*(*mn157*), *sod-2*(*gk257*); LGII: *damt-1*(*gk961032*); LGIII: *nmad-1*(*ok3133*), LGX: *sod-3*(*tm760*). In this paper, mutant worms were backcrossed: *damt-1*, 5–7 times; *nmad-1*, 5–9 times. Worms were grown on *dam*$^-$*dcm*$^-$ bacteria (NEB C2925) in all experiments except for Figure S1A, where they were grown on OP50-1 bacteria.

Fertility Assays

From day 3 to day 8 post-hatching, 10 worms were placed on NGM plates with bacteria in triplicate (30 worms total per condition). Worms were grown at 20°C. After 24 hr, the adult worms were removed from each plate and placed on new plates. The numbers of eggs and hatched worms on the plate were counted. Statistical analyses of fertility were performed using two-way ANOVA tests with Bonferroni post-tests or t tests using mean and standard error values.

Worm gDNA Extraction

Worms were washed two times with M9 buffer. 250 μl of worm genomic DNA lysis buffer (200 mM NaCl, 100 mM Tris-HCl [pH 8.5], 50 mM EDTA [pH 8.0],

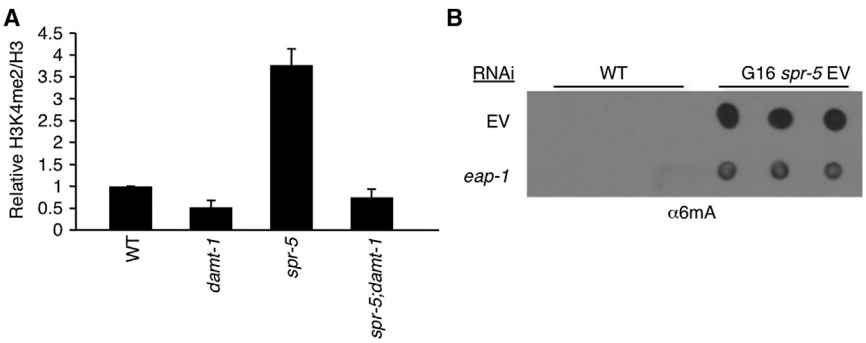

Figure 7. DNA Methylation and Histone Methylation Crosstalk

(A) Deletion of *damt-1* suppresses the elevated H3K4me2 levels of late-generation *spr-5*(*by134*) mutant worms. Each bar represents the mean ± SEM of three independent experiments performed in biological duplicate. Image J was used to analyze the relative intensity of H3K4me2 compared to histone H3. Western blots corresponding to two of these experiments are shown in Figures S7A and S7B.

(B) Knockdown of H3K9me binding protein, *eap-1*, suppresses the elevated 6mA level detected in *spr-5* mutant worms as assessed by dot blots. A longer exposure showing 6mA levels in WT worms is shown in Figure S7C.

0.5% SDS) + proteinase K (0.1 mg/ml) was added. Worms were incubated at 65°C for 1 hr with occasional vortexing and then incubated at 95°C for 20 min. RNase A was added (0.1 mg/ml) and incubated at 37°C for 1 hr. 250 μl of phenol;chloroform;isoamylic acid was added. Samples were mixed and then spun at 13,000 rpm at room temperature for 15 min. The aqueous phase was removed to a new tube, and phenol;chloroform;isoamylic acid extraction was repeated. To the aqueous phase, 25 μl of 3M sodium acetate and 750 μl of 100% EtOH were added and samples were placed at −80°C for at least 1 hr. Samples were spun at 13,000 rpm at 4°C for 30 min. The supernatant was removed. 350 μl of cold 75% EtOH was added, and samples were again spun at 13,000 rpm for 10 min. The supernatant was discarded, and pellet was allowed to dry before being resuspended in TE (10 mM Tris-HCl, 1 mM EDTA [pH 8.0, final pH 7.5]). For samples presented in Figures 7B, S1B, S4C, and S7C, purified gDNA was then treated with RNase A/T1 mix (Thermo Scientific) at a 1:20 dilution and RNaseH (NEB) at a 1:50 dilution for 1 hr at 37°C for 1 hr prior to subsequent re-purification starting with proteinase K digestion.

Dot Blot

Samples were diluted to 100 ng/μl and heated at 95°C for 10 min to denature DNA. Samples were immediately placed on ice for 5 min, and 250 ng were loaded per dot on Hybond + membranes. Membranes were allowed to air dry and placed in boxes with damp paper towels. DNA was then autocrosslinked in a UV stratalinker 2400 (Stratagene) two times. The membrane was allowed to dry and then blocked for 1 hr in 5% milk TBS. Membranes were probed for 1 hr at room temperature or overnight at 4°C with primary antibody in 5% milk TBS. Blots were washed three times for 10 min with TTBS and then probed with secondary antibody in 5% milk for 1 hr at room temperature. Blots were washed three times for 10 min with TTBS, and ECL was applied and film was developed.

SMRT Sequencing

The raw data are from two parts: (1) our own data, uploaded into GEO (accession number GSE66504) and (2) from PacBio public database (http://datasets.pacb.com.s3.amazonaws.com/2014/c_elegans/list.html). Each of the raw data in bax.h5 format were first aligned to ce10 genome using pbalign in base modification identification mode. The polymerase kinetics information was further loaded after alignment by loadChemistry.py and loadPulses scripts. Then two post-aligned datasets were merged and sorted by using cmph5tools. Finally, the 6mA was identified using ipdSummary.py script. We then further filtered 6mAs with less than 50× coverage. For motif identification, we first separated the whole 6mAs into 10 groups based on their methylation level (methylation level ranges: 0%–10%; 10%–20%…90%–100%). For each 6mA, we then extracted 2bp from the upstream and downstream sequences. MEME-ChIP (Machanick and Bailey, 2011) was then used to identify motifs in each group. The genome-wide 6mA and motif profiles are generated from circlize (Gu et al., 2014). Part of the analysis was done by customized scripts in R, Python, and Perl.

Antibodies

The following antibodies were used: α6mA (Synaptic Systems, 202 003), α6mA (Megabase Research), α5mC (Active Motif, 39649), α5hmC (Active Motif 39769), α3mC (Active Motif, 61111 and 61179), and α1mA (Active Motif, custom). α6mA (Megabase Research) was only used in Figure S1A.

SUPPLEMENTAL INFORMATION

Supplemental Information includes Extended Experimental Procedures and seven figures and can be found with this article online at http://dx.doi.org/10.1016/j.cell.2015.04.005.

AUTHOR CONTRIBUTIONS

E.L.G., M.A.B., and Y.S. conceived and planned the study and wrote the paper. E.L.G. produced Figures 1A, 3, 5A, 5D, 5F, 6, 7A, S1C, S3A, S4B, S4C, S6A, S7A, and S7B. M.A.B. produced Figures 1A, 4A, 4B, 4C, S1A, S1B, S1D, and S5A. L.G. performed bioinformatics analysis presented in Figures 2, S5B, and S5C. E.S. produced Figures 5B, 5C, 7B, S6C, and S7C. J.L. performed UHPLC-MS/MS experiments shown in Figures 1B, 4D, 5E, S1E, and S2 and was advised by C.H. D.A.-C. produced Figures 1C, 1D, S3B, and S4A. C.-H.H. performed protein purifications and DNA methylation assays. L.A. identified *damt-1* bioinformatically and produced Figures 5A and S6B.

ACKNOWLEDGMENTS

We thank members of the Shi lab for helpful discussions, Elizabeth Pollina for feedback on the manuscript, and Madeline Schuck and LaVondea Elow for technical and administrative support. We thank the Caenorhabditis Genetics Center, which is funded by NIH Office of Research Infrastructure Programs (P40OD010440) for *C. elegans* strains, and the Tufts University Core Facility Genomics Core and the University of Massachusetts Medical School Deep Sequencing Core for MeDIP-seq and SMRT sequencing, respectively. E.L.G. was supported by a Helen Hay Whitney postdoctoral fellowship and a National Institute on Aging of the NIH grant (K99AG043550). M.A.B. was supported by an NIH NRSA postdoctoral fellowship (1F32CA180450-01) and is currently supported by a Special Fellow award from the Leukemia & Lymphoma Society (3353-15). L.A. was supported by funds of the Intramural Research Program of the National Library of Health, NIH, and U.S. department of Health and Human Services. C.H. is a Howard Hughes Medical Institute investigator. This work was supported by NIH grants to Y.S. (GM058012, CA118487, and MH096066) and E.L.G. (K99AG043550), by an Ellison Foundation Senior Scholar Award to Y.S, and by a Samual Waxman Cancer Research Foundation grant to Y.S. (SWCRF-1856). Y.S. is an American Cancer Society Research Professor. Y.S. is also a cofounder of Constellation Pharmaceuticals Inc. and is a member of its scientific advisory board.

Received: November 8, 2014
Revised: March 2, 2015
Accepted: March 31, 2015
Published: April 30, 2015

REFERENCES

Anantharaman, V., Koonin, E.V., and Aravind, L. (2002). Comparative genomics and evolution of proteins involved in RNA metabolism. Nucleic Acids Res. *30*, 1427–1464.

Arber, W., and Dussoix, D. (1962). Host specificity of DNA produced by Escherichia coli. I. Host controlled modification of bacteriophage lambda. J. Mol. Biol. *5*, 18–36.

Benyshek, D.C., Johnston, C.S., and Martin, J.F. (2006). Glucose metabolism is altered in the adequately-nourished grand-offspring (F3 generation) of rats malnourished during gestation and perinatal life. Diabetologia *49*, 1117–1119.

Braun, R.E., and Wright, A. (1986). DNA methylation differentially enhances the expression of one of the two E. coli dnaA promoters in vivo and in vitro. Mol. Gen. Genet. *202*, 246–250.

Cavalli, G., and Paro, R. (1998). The Drosophila Fab-7 chromosomal element conveys epigenetic inheritance during mitosis and meiosis. Cell *93*, 505–518.

Clancy, M.J., Shambaugh, M.E., Timpte, C.S., and Bokar, J.A. (2002). Induction of sporulation in Saccharomyces cerevisiae leads to the formation of N6-methyladenosine in mRNA: a potential mechanism for the activity of the IME4 gene. Nucleic Acids Res. *30*, 4509–4518.

Csankovszki, G., Nagy, A., and Jaenisch, R. (2001). Synergism of Xist RNA, DNA methylation, and histone hypoacetylation in maintaining X chromosome inactivation. J. Cell Biol. *153*, 773–784.

Dias, B.G., and Ressler, K.J. (2014). Parental olfactory experience influences behavior and neural structure in subsequent generations. Nat. Neurosci. *17*, 89–96.

Dominissini, D., Moshitch-Moshkovitz, S., Schwartz, S., Salmon-Divon, M., Ungar, L., Osenberg, S., Cesarkas, K., Jacob-Hirsch, J., Amariglio, N., Kupiec, M., et al. (2012). Topology of the human and mouse m6A RNA methylomes revealed by m6A-seq. Nature *485*, 201–206.

Flusberg, B.A., Webster, D.R., Lee, J.H., Travers, K.J., Olivares, E.C., Clark, T.A., Korlach, J., and Turner, S.W. (2010). Direct detection of DNA methylation during single-molecule, real-time sequencing. Nat. Methods *7*, 461–465.

Fu, Y., Dominissini, D., Rechavi, G., and He, C. (2014). Gene expression regulation mediated through reversible m^{6}A RNA methylation. Nat. Rev. Genet. *15*, 293–306.

Fu, Y., Luo, G.-Z., Chen, K., Deng, X., Yu, M., Han, D., Hao, Z., Liu, J., Lu, X., Dore, L.C., et al. (2015). *N*^{6}-methyldeoxyadenosine marks active transcription start sites in *Chlamydomonas*. Cell *161*, this issue, ■■■–■■■.

Gao, F., Liu, X., Wu, X.P., Wang, X.L., Gong, D., Lu, H., Xia, Y., Song, Y., Wang, J., Du, J., et al. (2012). Differential DNA methylation in discrete developmental stages of the parasitic nematode Trichinella spiralis. Genome Biol. *13*, R100.

Gaydos, L.J., Wang, W., and Strome, S. (2014). Gene repression. H3K27me and PRC2 transmit a memory of repression across generations and during development. Science *345*, 1515–1518.

Greer, E.L., and Shi, Y. (2012). Histone methylation: a dynamic mark in health, disease and inheritance. Nat. Rev. Genet. *13*, 343–357.

Greer, E.L., Maures, T.J., Ucar, D., Hauswirth, A.G., Mancini, E., Lim, J.P., Benayoun, B.A., Shi, Y., and Brunet, A. (2011). Transgenerational epigenetic inheritance of longevity in Caenorhabditis elegans. Nature *479*, 365–371.

Greer, E.L., Beese-Sims, S.E., Brookes, E., Spadafora, R., Zhu, Y., Rothbart, S.B., Aristizabal-Corrales, D., Chen, S., Badeaux, A.I., Jin, Q., et al. (2014). A histone methylation network regulates transgenerational epigenetic memory in C. elegans. Cell Rep. *7*, 113–126.

Gu, Z., Gu, L., Eils, R., Schlesner, M., and Brors, B. (2014). circlize Implements and enhances circular visualization in R. Bioinformatics *30*, 2811–2812.

Gutiérrez, J.C., Callejas, S., Borniquel, S., and Martín-González, A. (2000). DNA methylation in ciliates: implications in differentiation processes. Int. Microbiol. *3*, 139–146.

Han, J.S., Kang, S., Kim, S.H., Ko, M.J., and Hwang, D.S. (2004). Binding of SeqA protein to hemi-methylated GATC sequences enhances their interaction and aggregation properties. J. Biol. Chem. *279*, 30236–30243.

Iyer, L.M., Abhiman, S., and Aravind, L. (2011). Natural history of eukaryotic DNA methylation systems. Prog. Mol. Biol. Transl. Sci. *101*, 25–104.

Iyer, L.M., Zhang, D., Burroughs, A.M., and Aravind, L. (2013). Computational identification of novel biochemical systems involved in oxidation, glycosylation and other complex modifications of bases in DNA. Nucleic Acids Res. *41*, 7635–7655.

Iyer, L.M., Zhang, D., de Souza, R.F., Pukkila, P.J., Rao, A., and Aravind, L. (2014). Lineage-specific expansions of TET/JBP genes and a new class of DNA transposons shape fungal genomic and epigenetic landscapes. Proc. Natl. Acad. Sci. USA *111*, 1676–1683.

Kato, M., Miura, A., Bender, J., Jacobsen, S.E., and Kakutani, T. (2003). Role of CG and non-CG methylation in immobilization of transposons in Arabidopsis. Curr. Bio. *13*, 421–426.

Katz, D.J., Edwards, T.M., Reinke, V., and Kelly, W.G. (2009). A C. elegans LSD1 demethylase contributes to germline immortality by reprogramming epigenetic memory. Cell *137*, 308–320.

Kerr, S.C., Ruppersburg, C.C., Francis, J.W., and Katz, D.J. (2014). SPR-5 and MET-2 function cooperatively to reestablish an epigenetic ground state during passage through the germ line. Proc. Natl. Acad. Sci. USA *111*, 9509–9514.

Klass, M., Nguyen, P.N., and Dechavigny, A. (1983). Age-correlated changes in the DNA template in the nematode Caenorhabditis elegans. Mech. Ageing Dev. *22*, 253–263.

Koh, K.P., and Rao, A. (2013). DNA methylation and methylcytosine oxidation in cell fate decisions. Curr. Opin. Cell Biol. *25*, 152–161.

Law, J.A., and Jacobsen, S.E. (2010). Establishing, maintaining and modifying DNA methylation patterns in plants and animals. Nat. Rev. Genet. *11*, 204–220.

Liu, N., Dai, Q., Zheng, G., He, C., Parisien, M., and Pan, T. (2015). N(6)-methyladenosine-dependent RNA structural switches regulate RNA-protein interactions. Nature *518*, 560–564.

Machanick, P., and Bailey, T.L. (2011). MEME-ChIP: motif analysis of large DNA datasets. Bioinformatics *27*, 1696–1697.

Martin, C., and Zhang, Y. (2007). Mechanisms of epigenetic inheritance. Curr. Opin. Cell Biol. *19*, 266–272.

Meselson, M., and Yuan, R. (1968). DNA restriction enzyme from E. coli. Nature *217*, 1110–1114.

Moazed, D. (2011). Mechanisms for the inheritance of chromatin states. Cell *146*, 510–518.

Morgan, H.D., Sutherland, H.G., Martin, D.I., and Whitelaw, E. (1999). Epigenetic inheritance at the agouti locus in the mouse. Nat. Genet. *23*, 314–318.

Nottke, A.C., Beese-Sims, S.E., Pantalena, L.F., Reinke, V., Shi, Y., and Colaiácovo, M.P. (2011). SPR-5 is a histone H3K4 demethylase with a role in meiotic double-strand break repair. Proc. Natl. Acad. Sci. USA *108*, 12805–12810.

Rechavi, O., Houri-Ze'evi, L., Anava, S., Goh, W.S., Kerk, S.Y., Hannon, G.J., and Hobert, O. (2014). Starvation-induced transgenerational inheritance of small RNAs in C. elegans. Cell *158*, 277–287.

Sado, T., Fenner, M.H., Tan, S.S., Tam, P., Shioda, T., and Li, E. (2000). X inactivation in the mouse embryo deficient for Dnmt1: distinct effect of hypomethylation on imprinted and random X inactivation. Dev. Biol. *225*, 294–303.

Saksouk, N., Barth, T.K., Ziegler-Birling, C., Olova, N., Nowak, A., Rey, E., Mateos-Langerak, J., Urbach, S., Reik, W., Torres-Padilla, M.E., et al. (2014). Redundant mechanisms to form silent chromatin at pericentromeric regions rely on BEND3 and DNA methylation. Mol. Cell *56*, 580–594.

Shi, Y., Lan, F., Matson, C., Mulligan, P., Whetstine, J.R., Cole, P.A., Casero, R.A., and Shi, Y. (2004). Histone demethylation mediated by the nuclear amine oxidase homolog LSD1. Cell *119*, 941–953.

Simpson, V.J., Johnson, T.E., and Hammen, R.F. (1986). Caenorhabditis elegans DNA does not contain 5-methylcytosine at any time during development or aging. Nucleic Acids Res. *14*, 6711–6719.

Smith, Z.D., and Meissner, A. (2013). DNA methylation: roles in mammalian development. Nat. Rev. Genet. *14*, 204–220.

Stadler, M.B., Murr, R., Burger, L., Ivanek, R., Lienert, F., Schöler, A., van Nimwegen, E., Wirbelauer, C., Oakeley, E.J., Gaidatzis, D., et al. (2011). DNA-binding factors shape the mouse methylome at distal regulatory regions. Nature *480*, 490–495.

Stein, R., Razin, A., and Cedar, H. (1982). In vitro methylation of the hamster adenine phosphoribosyltransferase gene inhibits its expression in mouse L cells. Proc. Natl. Acad. Sci. USA *79*, 3418–3422.

Teixeira, F.K., Heredia, F., Sarazin, A., Roudier, F., Boccara, M., Ciaudo, C., Cruaud, C., Poulain, J., Berdasco, M., Fraga, M.F., et al. (2009). A role for RNAi in the selective correction of DNA methylation defects. Science *323*, 1600–1604.

Wassenegger, M., Heimes, S., Riedel, L., and Sänger, H.L. (1994). RNA-directed de novo methylation of genomic sequences in plants. Cell *76*, 567–576.

Wenzel, D., Palladino, F., and Jedrusik-Bode, M. (2011). Epigenetics in C. elegans: facts and challenges. Genesis *49*, 647–661.

Wion, D., and Casadesús, J. (2006). N6-methyl-adenine: an epigenetic signal for DNA-protein interactions. Nat. Rev. Microbiol. *4*, 183–192.

Yi, C., and He, C. (2013). DNA repair by reversal of DNA damage. Cold Spring Harb. Perspect. Biol. *5*, a012575.

Zemach, A., and Zilberman, D. (2010). Evolution of eukaryotic DNA methylation and the pursuit of safer sex. Curr. Bio. *20*, R780–R785.

Zemach, A., McDaniel, I.E., Silva, P., and Zilberman, D. (2010). Genome-wide evolutionary analysis of eukaryotic DNA methylation. Science *328*, 916–919.

Cell

EXTENDED EXPERIMENTAL PROCEDURES

Worm Strains

Generation 1 *spr-5* mutant worms were obtained by crossing later generation (generation 10-20) homozygous mutant worms with wild-type males to obtain P0 heterozygous mutants. Individual P0 heterozygous mutants were picked to plates and allowed to lay generation 1 progeny after which the P0 heterozygous mutant genotype was confirmed by single worm PCR genotyping. Generation 1 progeny were picked to individual plates and allowed to lay progeny. Generation 1 worms were subsequently genotyped by single worm PCR and homozygous mutant worms were perpetuated for subsequent generations. For double mutant crosses WT males were crossed with either *spr-5* or second mutant homozygous mutant hermaphrodites. Male progeny from these crosses were then crossed with homozygous mutant or *spr-5* hermaphrodites, respectively. Hermaphrodite progeny from these crosses were picked to individual plates and allowed to lay progeny. The parental generation was then genotyped by single worm PCR at the mutant loci used in the male strain. Progeny of heterozygous parental generation worms were picked to individual plates and after laying progeny were genotyped at both mutant loci. Subsequent single or double homozygous mutant progeny were maintained until the appropriate generation and egg laying assays or gDNA analyses were performed.

RNA Interference

dam^{-}*dcm*$^{-}$ bacteria (NEB C2925) transformed with vectors expressing dsRNA of *damt-1* were obtained from the Ahringer library (a gift from T.K. Blackwell). *dam*$^{-}$*dcm*$^{-}$ bacteria containing the vectors of interest were grown at 37°C and seeded on standard nematode growth medium (NGM) plates containing ampicillin (100 mg ml^{-1}) and isopropylthiogalactoside (IPTG; 0.4 mM).

Whole-Mount Immunocytochemistry

For whole worm immunostaining, worms were washed several times to remove bacteria and resuspended in fixing solution (160 mM KCl, 40 mM NaCl, 20 mM Na_2EGTA, 10 mM spermidine HCl, 30 mM PIPES pH 7.4, 50% methanol, 2% β-mercaptoethanol, 2% formaldehyde) and subjected to two rounds of snap freezing in liquid N_2. The worms were fixed at 4°C for 30 min and washed two times briefly in T buffer (100 mM Tris-HCl pH7.4, 1 mM EDTA, 1% Triton X-100) before a 1 hr incubation in T buffer supplemented with 1% β-mercaptoethanol at 37°C. The worms were washed with borate buffer (25 mM H_3BO_3, 12.5 mM NaOH pH 9.5) and then washed in 1x PBS to equilibrate pH for RNase treatment. Worms were incubated at 37°C with a 1:100 RNase A/T1 mix (thermo scientific) in PBS for 2 hr. Worms were washed in borate buffer and then incubated in borate buffer containing 10 mM DTT for 15 min. Worms were washed with borate buffer and then incubated in borate buffer containing 0.3% H_2O_2. Worms were washed in borate buffer briefly and then were blocked in PBST (PBS pH 7.4, 1% BSA, 0.5% Triton X-100, 5 mM sodium azide, 1 mM EDTA) for 1 hr and then incubated overnight with 6mA antibody (1:100 in PBST). Worms were washed 4 times for 25 min in PBST and then incubated with Alexa Fluoro 588 secondary antibody (1:50 in PBST). Worms were washed 4 times for 25 min in PBST. DAPI (2 mg ml^{-1}) was added to visualize nuclei. The worms were mounted on a microscope slide and visualized using a Zeiss LSM700 confocal system.

Gonad Dissection, Immunohistochemistry, and Analysis

Worms were immobilized in 300 μl of 0.5 mM Levamisole in pyrex glass multiwells. Gonads were dissected out from young adult hermaphrodites (24 hr post-L4) and fixed by adding 500 μl of 2% FA/WB solution (2% Formaldehyde, 1% B-mercaptoethoanol, 1x Witches Brew (1X Witches Brew: 80 mM KCl, 20 mM NaCl, 10 mM Na_2EGTA, 5 mM Spermidine, 15 mM NaPipes pH 7.4, 25% Methanol)). Worms were fixed for 30 min at room temperature. 2 washes with 500 μl of PBS-T (0.1% Tween in PBS) were performed followed by RNase digestion. RNase digestion using 200 μl of RNase A/T1 mix (Thermo Scientific) 1:20 in PBS with 80 mM HEPES pH 7.5 for 2-3 hr at 37°C. Gonads were washed with PBS-T and then incubated with 2N HCl for 20 min at room temperature to denature the DNA followed by neutralization with 100 mM Tris-HCl pH 8.5 for 10 min. Prior to antibody incubation, gonads were blocked in PBS-TB (0.1% Tween, 1% BSA in PBS) for one hour and then incubated in anti-6mA antibody (Synaptic Systems) at 1:100 overnight at 4°C. The next day, gonads were washed 4x with PBS-TB for 10 min and incubated for 2 hr at room temperature with goat anti-Rabbit Alexa 594 at 1:400 dilution. Finally gonads were washed 3x with PBS-TB before incubating with PBS-TB + DAPI for 10 min. For microscope observation gonads were placed on coverslide with vectashield and visualized for staining.

Single-Worm Genotyping

Single worms were placed in 5 μl of worm lysis buffer (50 mM KCl, 10 mM Tris pH 8.3, 2.5 mM $MgCl_2$, 0.45% NP40, 0.45% Tween-20, 0.01% gelatin (w/v) and 60 mg ml^{-1} proteinase K), and incubated at −80°C for 1 hr, 60°C for 1 hr, and then 95°C for 15 min. PCR reactions were performed using the following primers: damt-1 F: 5′- CGGTTATGGAGGAAAGAAGAAGGG-3′, damt-1 R: 5′- TTTTATGGGTATCGGGAACGG-3′, damt-1 I 5′- GCACATCCCAGGAATGAGATTG-3′, nmad-1 F: 5′- GGTTGAACAAGGAGAAG AATGACAAAACAG-3′, nmad-1 R: 5′- ATCCACCTCGTGCCAATCCG-3′, spr-5 (by101) F: 5′-AACACGTGCCTCCATGAATATCT-3′, spr-5 (by101) R: 5′-GAACACGTGTGTTCTCCAGCAA-3′, spr-5 (by101) I: 5′-CCTATAGAACTTTCCCACAGTG-3′, spr-5 (by134) F: 5′-CCAATTGTGCTCCAACC-3′, spr-5 (by134) R: 5′-AACTTCGAAGAGCACGGA-3′ (PCR reactions for spr-5(by134) were cut with PsiI to distinguish wild-type from mutant genotype). PCR reactions were performed according to the manufacturer's protocol (Invitrogen: Platinum PCR supermix) and PCR reactions were resolved on agarose gels.

Oligos Used for Antibody Validation and Demethylation Reactions

Regular or premethylated HPLC-purified oligos of the following sequences were purchased from The Midland Certified Reagent Company, Inc:

Oligo name	Oligo sequence
6mA	5′-GGGAATTTCCCGGCGATTTGA(N6-Me-dA)TCAA ATCGCCGGGAAATTCCC-3′
6A	5′-GGGAATTTCCCGGCGATTTGATCAA ATCGCCGGGAAATTCCC-3′
1mA	5′-GGGAATTTCCCGGCGATTTGA(N1-Me-dA)TCCC GGATCCCGTGGAGGCCC-3′
1A	5′-GGGAATTTCCCGGCGATTTGATCCC GGATCCCGTGGAGGCCC-3′
3mC	5′-GATTGGAAAGCAC(N3-Me-dC)GGTCGA AAAAGCGAAACTAGCTCTGACGTGC-3′
3C	5′-GATTGGAAAGCACGGTCGA AAAAGCGAAACTAGCTCTGACGTGC-3′

Quantification of 6mA in Genomic DNA by UHPLC-QQQ-MS/MS Analysis

Worm genomic DNA (1−4 μg) in 26 μl of nuclease-free H_2O was denatured at 100°C for 3 min, chilled on ice for 2 min, and digested by 1 μl nuclease P1 (1U/ μl, Wako USA) in 10 mM NH_4OAc pH 5.3 (adding 3 μl 100 mM NH_4OAc) at 42°C overnight. It was followed by addition of 3.4 μl NH_4HCO_3 (1 M) and 1 μl of phosphodiesterase I from crotalus adamanteus venom (0.001 U, Sigma-Aldrich) at 37°C for 2 hr and finally by addition of 1 U of alkaline phosphatase from *E.coli* (Sigma-Aldrich) at 37°C for 2 hr. Digested DNA was diluted two fold with nuclease-free H_2O. The diluted solution was filtered through 0.22 μm filter and 10 μl solution was injected into LC-MS/MS. The nucleosides were separated by reverse phase ultra-high performance liquid chromatography (UHPLC) on a C18 column (Agilent), with online mass spectrometry detection using Agilent 6460 QQQ triple-quadrupole tandem mass spectrometer (MS/MS) set to multiple reaction monitoring (MRM) in positive electrospray ionization mode. Nucleosides were quantified using the nucleoside precursor ion to base ion mass transitions of 266.1-150.0 for m^6dA and 252.1-136.0 for A. Quantification of the ratio 6mA/A was performed using the calibration curves obtained from nucleoside standards running at the same time.

Real-Time RT PCR

RNA was extracted by addition of 1 ml of Trizol (Invitrogen) for 100 μl of worm pellets of young adult worms. Six freeze thaw cycles were performed in liquid nitrogen. The RNA extraction was performed according to the Trizol protocol. The expression of target genes was determined by reverse transcription of 1 μg of total RNA with the Superscript III kit (Invitrogen) followed by quantitative PCR analysis on a Roche Lightcycler 480 II with SYBR Green I Master (Roche) with the following primers: *pan-actin* F: TCGGTATG GGACAGAAGGAC; pan-actin R: CATCCCAGTTGGTGACGATA; Y51H7C.5 F: TGAAAGAAGTGGCACGAGAAATG; Y51H7C.5 R: TGATTGGAGCAGCGAAGAGC; Y46G5A.35 F: TGAGCAACGAAAATGGCGAG; Y46G5A.35 R: ATAATAGCGTCGGAGAG CAGGG; C14B1.10 F: TTGGAGAGCGGTTTGAAGGAG; C14B1.10 R: GGATACTGCTATTGCTGACGAGAAG; B0564.2 F: CATCA AAAAGTTCATCGTCAAAAGC; B0564.2 R: TTGGTCATCAAGTATTTCAGTTCCAC; nmad-1 F: nmad-1R:. The results were expressed as $2^{(-(\text{Gene of interest number of cycles} - \text{actin number of cycles}))}$. Control PCR reactions were also performed on total RNA that had not been reverse-transcribed to test for the presence of genomic DNA in the RNA preparation.

MMS Treatment

Bacteria was washed several times and resuspended in S-basal (5.85 g NaCl, 1 g K_2HPO_4, 6 g KH_2PO_4 in 1L and sterilized) containing cholesterol (5 mg/l) and antibiotics. Worms were grown in liquid media in a gently shaking flask at room temperature. Worms were grown in various concentrations of MMS for 4 hr while shaking and then gDNA was extracted as above.

MeDIP-Seq

3-6 μgs of purified *C. elegans* genomic DNA were fragmented to 200-400 bp using a Bioruptor Standard. Illumina adaptors were ligated onto gDNA fragments as per the NEBNext DNA Library Prep Master Mix Set for Illumina kit protocol. Input adaptor-ligated DNA fragments were heat-denatured and immunoprecipitated overnight at 4°C, and anti-6mA-bound DNA was purified as per the Active Motif hMeDIP kit protocol (using 2 μg of anti-6mA (Synaptic Systems) antibody). Input and 6mA immunoprecipitated DNA was PCR amplified using Illumina Indexing primers, and multiplexed libraries were subjected to next generation sequencing. The raw data were aligned to ce10 genome using bwa-0.7.12 (Li and Durbin, 2009). Duplicated reads and reads mapped to more than one position were removed by samtools (Li et al., 2009) and Picard (http://picard.sourceforge.net.). The MEDIPS (Lienhard

et al., 2014) R package was then used for the saturation analysis to reach a sufficient coverage for each sample. The post-aligned datasets were further transformed into bigwig format for the profile visualization. Peak calling was further performed using macs2 (Zhang et al., 2008) callpeak function with the input data and the following options: -B–nomodel–SPMR. For motif analysis, we extracted 20bp from the upstream and downstream sequences of the summit of each conserved peak and used MEME-ChIP (Machanick and Bailey, 2011) to identify possible motifs enriched in each group. Part of the analysis was done by customized scripts in R, Python and Perl.

Demethylase Assays

Demethylation reactions were performed in a minimum of triplicate in 50 μl volumes containing 0.1 nmol oligo substrate and 1 μg recombinant protein in a reaction mixture consisting of 50 μM HEPES (pH 7.0), 50 μM KCl, 2 mM $MgCl_2$, 2 mM ascorbic acid, 1 mM α-KG, and 200 μM $(NH)_4Fe(SO)_4$. Reactions were performed for 1 hr at 37°C and stopped by addition of 5 mM EDTA followed by heating at 95°C for 10 min. 2 μl of reaction product was used for dot blotting as described above.

Phylogeny Tree

Sequences of the circularly permuted N6 methyltransferases clade to span a comprehensive phyletic range of eukaryotes and their closest prokaryotic homologs were collected using the PSI-BLAST program. The methylase domains were aligned using the MUSCLE program. The tree was constructed using two methods: 1) A preliminary tree was obtained using the approximately-maximum-likelihood method implemented in the FastTree 2.1 program under default parameters. This gave an idea of the relationships of the major clades. 2) A complete tree was constructed using the MEGA 5.1 program with the following parameters: 4 distinct gamma distributed rate categories and one invariant were used for modeling among site variation, the WAG matrix with frequencies, was used as the substitution model; the ML searched used the close neighbor exchange method. The tree was bootstrapped using 10,000 RELL-BP resamplings with the Molphy package. Both topologies were nearly congruent with all the major clades being recovered. The latter tree is shown with all branches where both methods wielded > 85% support being marked by a pink dot.

SUPPLEMENTAL REFERENCES

Li, H., and Durbin, R. (2009). Fast and accurate short read alignment with Burrows-Wheeler transform. Bioinformatics *25*, 1754–1760.

Li, H., Handsaker, B., Wysoker, A., Fennell, T., Ruan, J., Homer, N., Marth, G., Abecasis, G., and Durbin, R.; 1000 Genome Project Data Processing Subgroup (2009). The Sequence Alignment/Map format and SAMtools. Bioinformatics *25*, 2078–2079.

Lienhard, M., Grimm, C., Morkel, M., Herwig, R., and Chavez, L. (2014). MEDIPS: genome-wide differential coverage analysis of sequencing data derived from DNA enrichment experiments. Bioinformatics *30*, 284–286.

Zhang, Y., Liu, T., Meyer, C.A., Eeckhoute, J., Johnson, D.S., Bernstein, B.E., Nusbaum, C., Myers, R.M., Brown, M., Li, W., and Liu, X.S. (2008). Model-based analysis of ChIP-Seq (MACS). Genome Biol. *9*, R137.

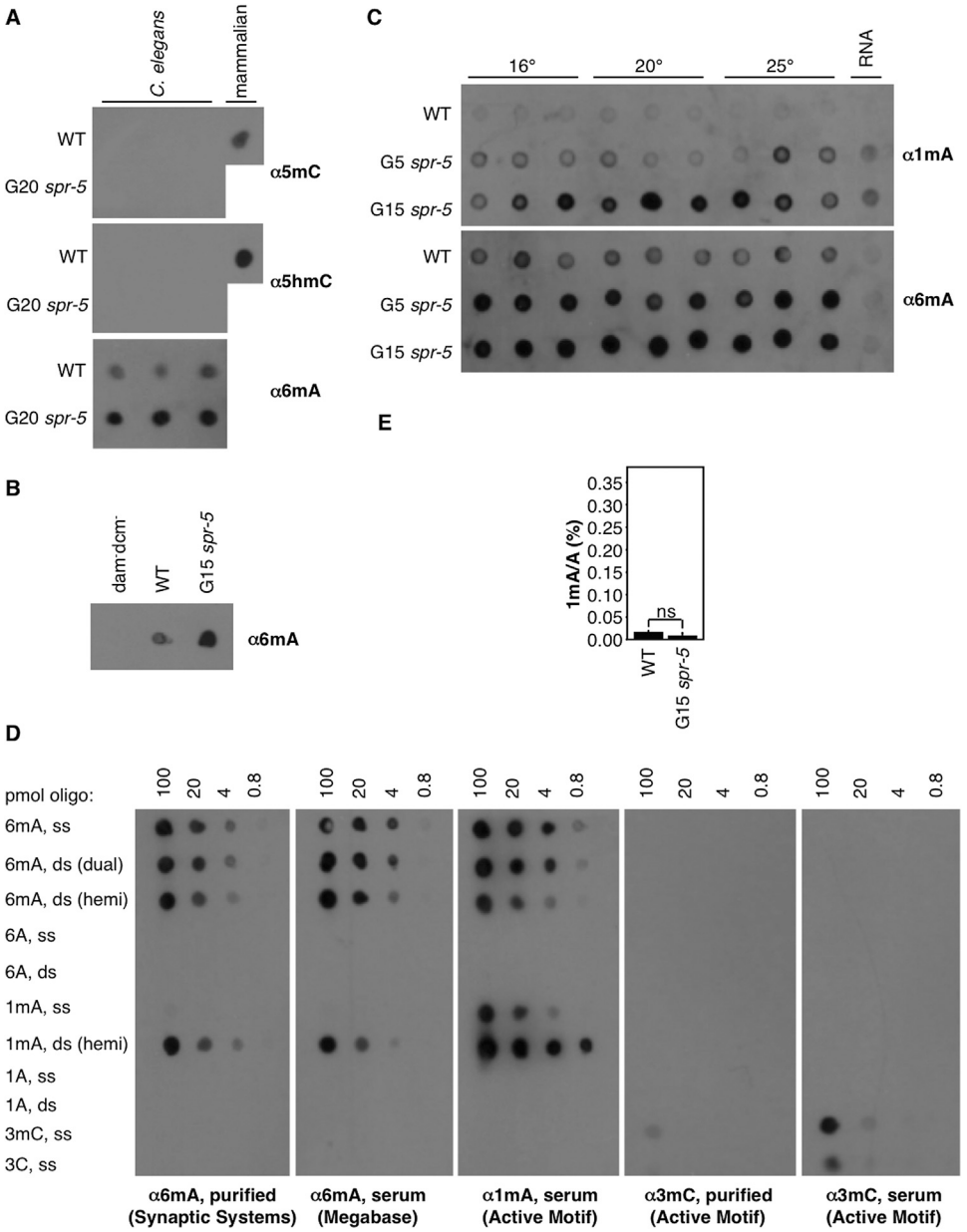

Figure S1. Controls for 6mA Detection in *C. elegans*, Related to Figure 1

(A) Dot blots of 3 biological replicates of WT and generation 20 *spr-5(by101)* mutant worms show elevated 6mA levels with no detectable 5mC or 5hmC. 250 ng of gDNA are loaded per dot. Mammalian gDNA is used as a control for 5mC and 5hmC antibody strength.

(B) Dot blots of 250 ngs of *dam*$^{-}$*dcm*$^{-}$ bacteria as well as WT and G15 *spr-5(by101)* mutant worms that were fed *dam*$^{-}$*dcm*$^{-}$ bacteria. No detectable 6mA was found in the *dam*$^{-}$*dcm*$^{-}$ bacterial food source. *dam*$^{-}$*dcm*$^{-}$ bacteria gDNA, if present in the worm intestine, would be at much lower relative concentrations than worm gDNA. Purified worm gDNA samples were digested with RNase A/T1 and RNaseH to remove any residual RNA from the samples.

(C) Dot blots of 3 biological replicates of WT, generation 5, and generation 15 *spr-5(by101)* mutant worms grown at 16°, 20°, or 25° all show progressively elevated signal using the 1mA antibody that recognizes both 1mA and 6mA. 6mA blot is a longer exposure of blot in Figure 1A. 250 ng of gDNA are loaded per dot.

(D) Serial dilution of 6mA, 1mA, and 3mC premethylated and unmethylated oligos show the specificity of the DNA methylation antibodies used in this study. Both 6mA antibodies are specific to 6mA-methylated DNA but also detect double stranded non-denatured 1mA oligos. The 1mA antibody recognizes both 6mA and 1mA methylated oligos. The 3mC antibody has a ~5 fold higher recognition of methylated versus unmethylated DNA oligos. ss: single stranded denatured oligos; ds: double stranded non-denatured oligos; hemi: hemi-methylated oligos; dual: both oligo strands are methylated.

(E) 1mA levels do not increase in late generation *spr-5(by101)* mutant worms as assessed by UHPLC-MS/MS. Each column represents the mean and standard deviation of 3-5 biological replicates per group.

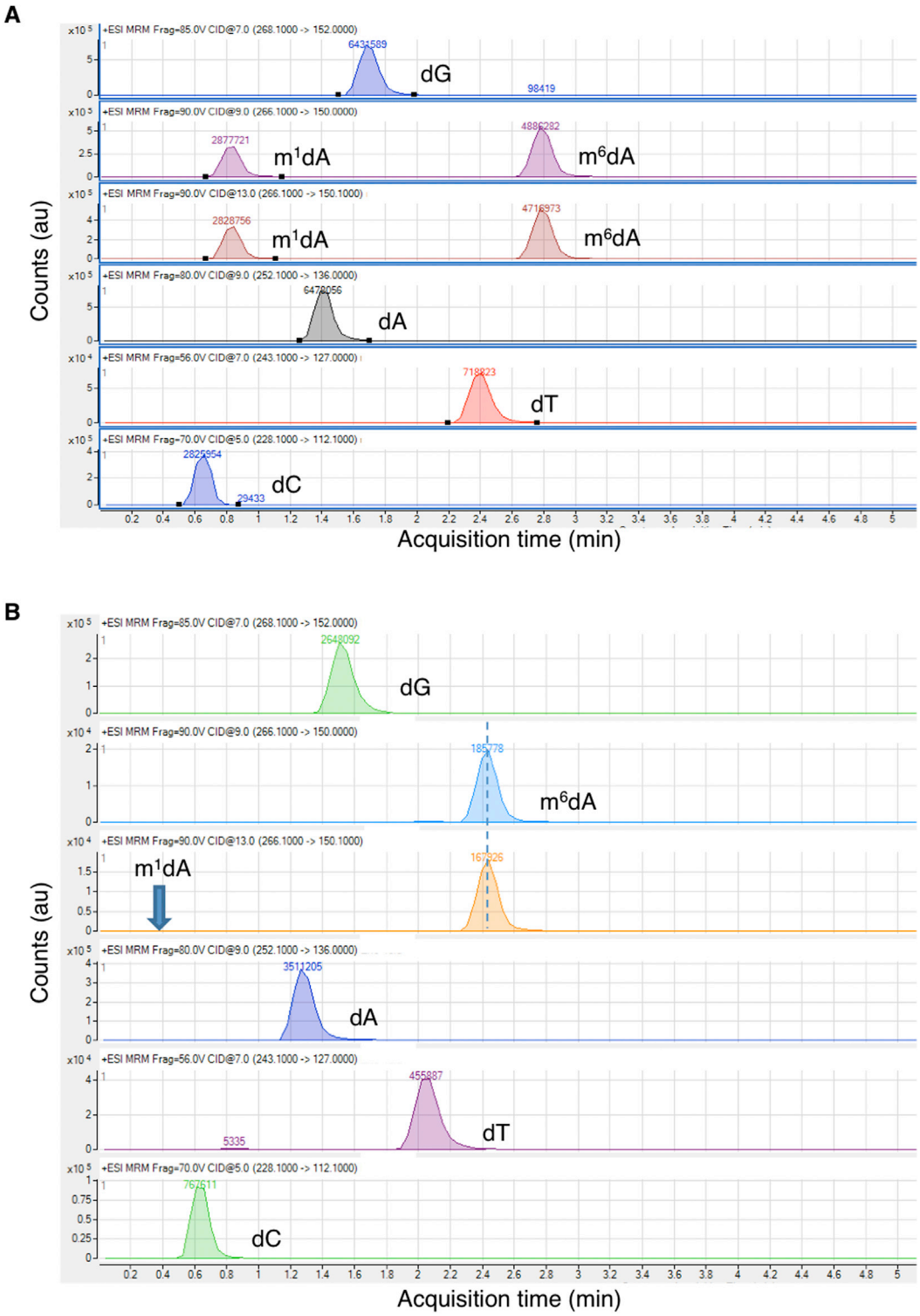

Figure S2. Example MS Spectra, Related to Figure 1

(A) Nucleoside standards representing all different bases including 1mA and 6mA.

(B) Representative MS spectra of *C. elegans* genomic DNA. These spectra demonstrate where 6mA appears compared to 1mA. There are slight variations from run to run due to column and flow rate differences but the peak order is consistent.

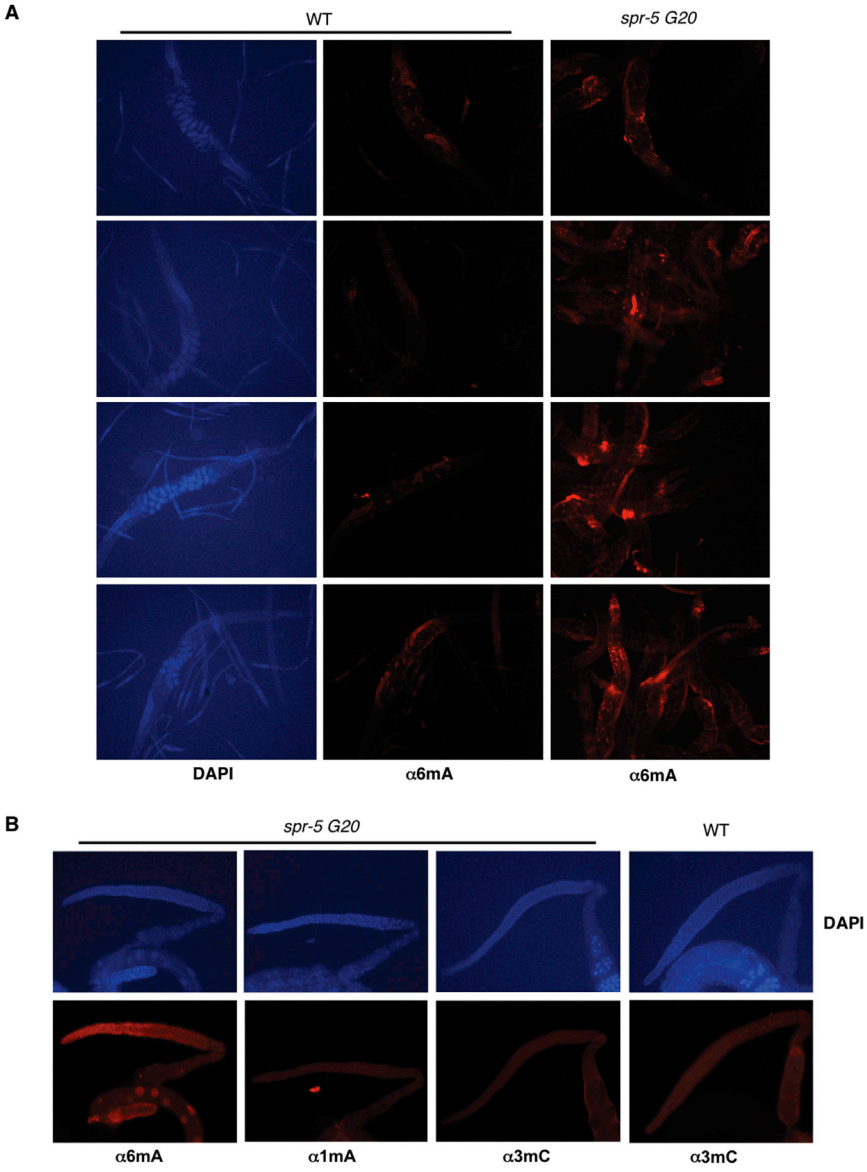

Figure S3. Whole-Worm and Extracted Germline Immunofluorescence, Related to Figure 1

(A) Whole mount worm immunofluorescence shows variable levels of 6mA in independent worm samples. Late generation *spr-5(by101)* mutant worms show ubiquitously increased 6mA levels. DAPI staining was blunted by 6mA staining protocol so was not achievable in some samples.

(B) *spr-5(by101)* extracted worm germlines do not show elevated 3mC levels, and 1mA signal is diffuse and at background levels.

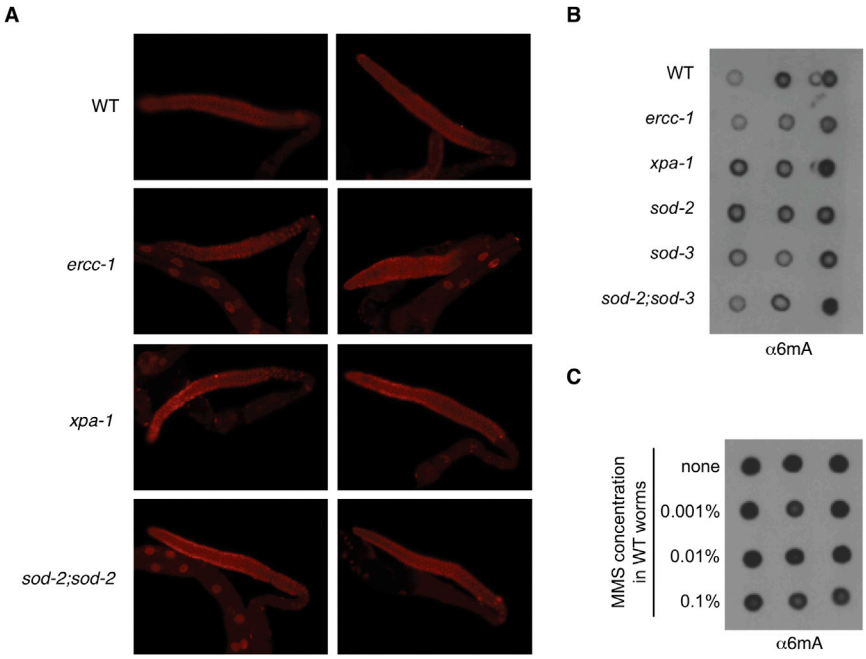

Figure S4. DNA Damage Mutants Do Not Affect 6mA Staining in Extracted Gonads, Related to Figure 1

(A) Immunofluorescence shows that extracted gonads of DNA damage mutants *ercc-1*, *xpa-1*, and *sod-2;sod-3* do not have appreciably elevated 6mA levels compared with extracted gonads of WT worms.

(B) Dot blots of gDNA extracted from WT and DNA damage mutants show that DNA damage mutants do not have elevated levels of 6mA compared with WT worms.

(C) Increasing concentrations of the DNA damaging agent methyl methanesulfonate (MMS) do not increase 6mA levels in WT worms. Worms were treated for 4 hr with MMS. The highest concentration of MMS had begun to kill ~10% of the worm population at this time.

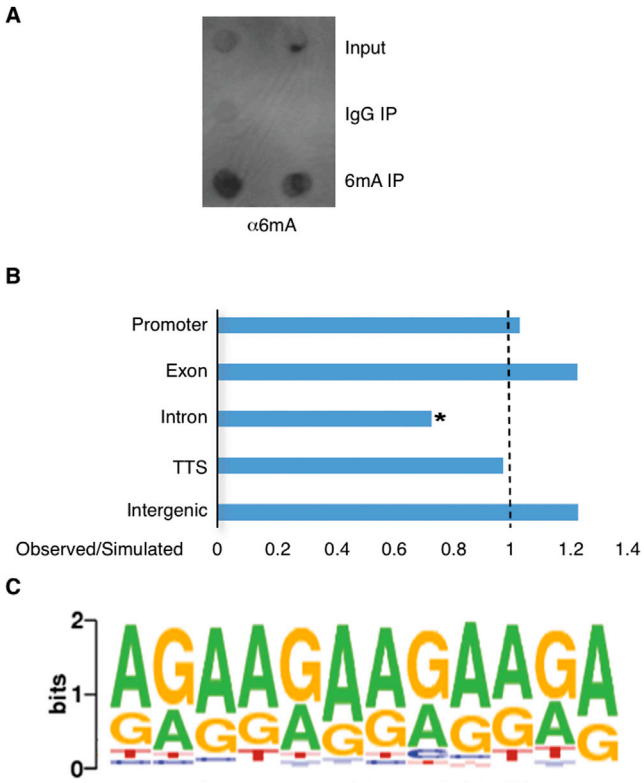

Figure S5. 6mA MeDIP-Seq, Related to Figure 2

(A) 6mA DNA immunoprecipitation (IP) of WT worm gDNA enriched 6mA methylated DNA as detected by dot blots of duplicate IPs. Input and IP samples were normalized to the same concentration; concentrations of IgG IPs were too low to be accurately measured.

(B) Comparison of observed versus simulated distributions of 6mA across the *C. elegans* genome as determined by MeDIP-seq of WT worms. *$p < 0.01$.

(C) MeDIP-seq identified eleven motifs associated with 6mA. The most significant one, displayed here, occurred in 314 of the 766 peaks identified ($p = 1e\text{-}42$).

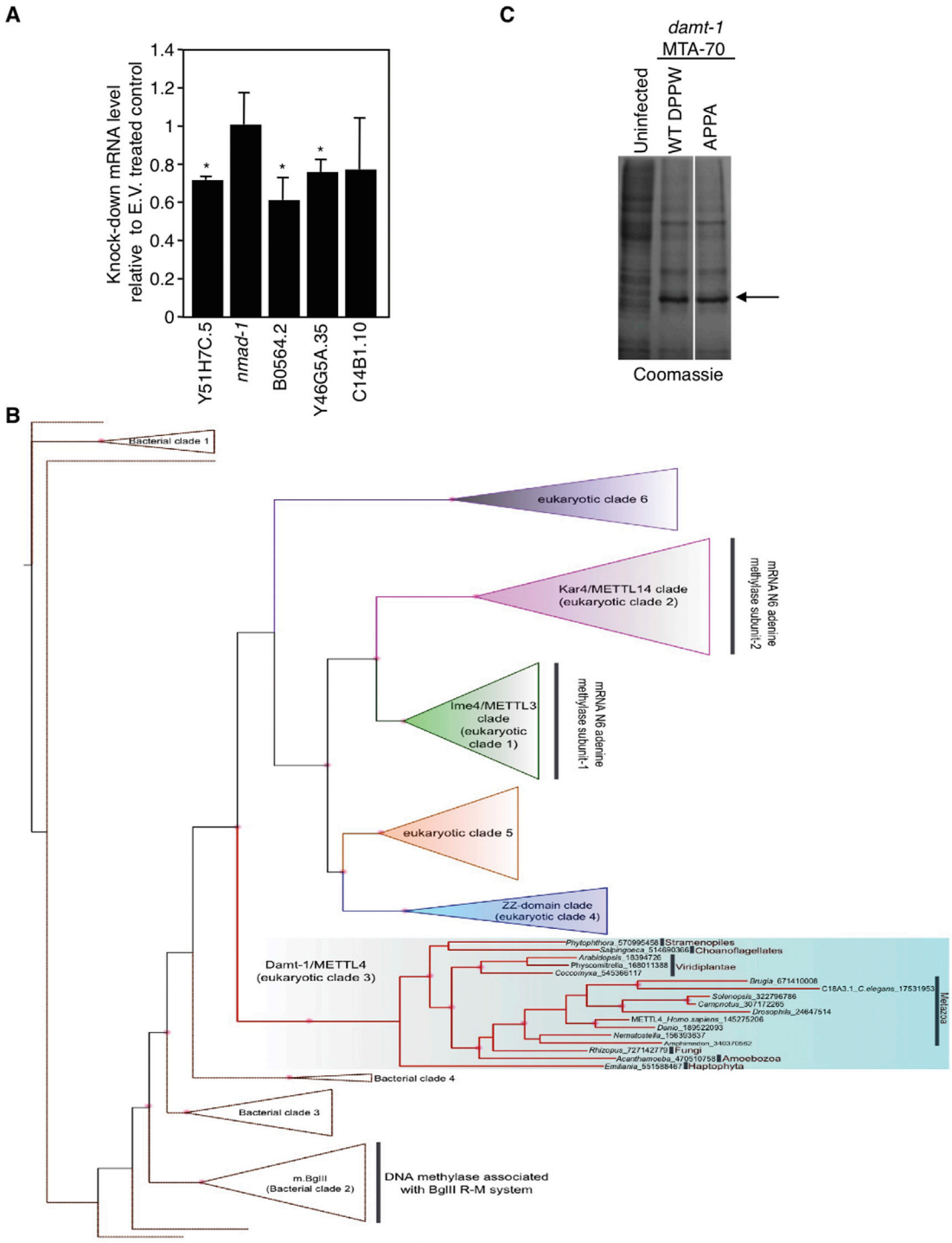

Figure S6. Knockdown of ALKBH Family Members, DAMT-1 Family Tree, and DAMT-1 Expression in SF9 Cells, Related to Figures 3 and 5

(A) Knockdown efficiency of bacteria expressing dsRNA against ALKBH family members as assessed by real-time RT PCR. Knockdown of *nmad-1* showed no detectable difference in *nmad-1* mRNA levels. *$p < 0.05$. Related to Figure 3.

(B) The expanded phylogenetic tree from Figure 5A is shown. The bacterial clades which form successive outgroups of the eukaryotic clades are colored brown. Each eukaryotic clade is labeled and the individual representatives of the Damt-1/METTL4 clade are labeled using the genus name followed by NCBI GenBank Identifier. The phyletic patterns are indicated to the extreme right for representatives of this clade.

(C) Coomassie staining of SF9 whole cell lysates shows that WT and APPA mutated DAMT-1 MTA-70 domains are expressed at similar levels in SF9 cells. Related to Figure 5C.

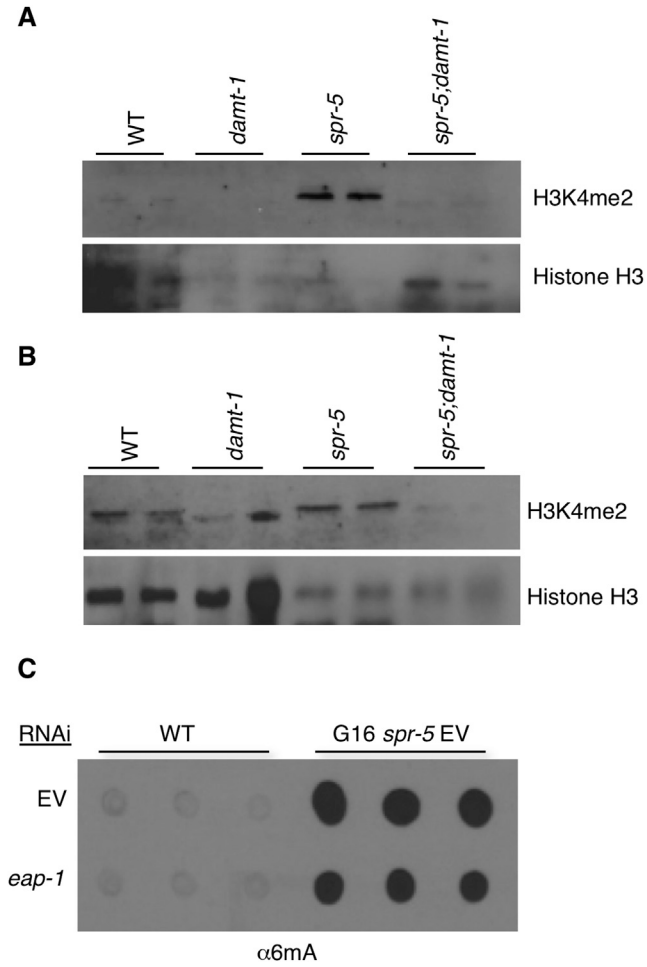

Figure S7. DNA and Histone Methylation Crosstalk

(A and B) Late generation *spr-5(by134)* mutant worms have elevated levels of H3K4me2, which was suppressed in equivalent generation *spr-5;damt-1* double mutants. A and B show different blots of the same samples. Average quantification is displayed in Figure 7A.

(C) Knockdown of H3K9me binding protein, *eap-1*, suppresses the elevated 6mA level detected in *spr-5* mutant worms but had no appreciable effect on WT worms as assessed by dot blots. A lower exposure showing 6mA levels in *spr-5* mutant worms is shown in Figure 7B.